



HAL
open science

Modelling, simulation and mathematical analysis of drone swarms via entropy methods

Claudia Negulescu, Axel Maupoux, Etienne Lehman

► **To cite this version:**

Claudia Negulescu, Axel Maupoux, Etienne Lehman. Modelling, simulation and mathematical analysis of drone swarms via entropy methods. 2023. hal-03721608v2

HAL Id: hal-03721608

<https://hal.science/hal-03721608v2>

Preprint submitted on 3 Jul 2023

HAL is a multi-disciplinary open access archive for the deposit and dissemination of scientific research documents, whether they are published or not. The documents may come from teaching and research institutions in France or abroad, or from public or private research centers.

L'archive ouverte pluridisciplinaire **HAL**, est destinée au dépôt et à la diffusion de documents scientifiques de niveau recherche, publiés ou non, émanant des établissements d'enseignement et de recherche français ou étrangers, des laboratoires publics ou privés.

Modelling, simulation and mathematical analysis of drone swarms via entropy methods

Dolomiti summer school 2021

Le Tre Cime di Lavaredo Summer School on Applied Mathematics



Claudia NEGULESCU

Axel MAUPOUX, Etienne LEHMAN

UNIVERSITÉ Paul Sabatier, Toulouse III

Institut de Mathématiques de Toulouse

Équipe: Équations aux Dérivées Partielles

Unité Mixte de Recherches CNRS - Université Paul Sabatier Toulouse 3 - INSA Toulouse - Université Toulouse 1

UMR 5219

Université Paul Sabatier Toulouse 3, 118 route de Narbonne, 31062 TOULOUSE cédex 9, France

Foreword

These notes summarize a series of lectures given by Claudia Negulescu at the Institut supérieur de l'aéronautique et de l'espace (ISAE-SUPAERO) during the years 2019-2022. They are devoted to an elementary and self-consistent approach of the mathematical theory emerging in the modelling of the collective behaviour of certain natural phenomena. The notion of entropy plays here a crucial role, in particular entropy dissipative techniques are the basis for the investigation of the qualitative behaviour of nonlinear PDEs.

The lectures are based on published works, which were specifically chosen to illustrate different techniques in the field of collective behaviour. The writing was facilitated by a very careful and critical reading of the manuscript by the two PhD students of Claudia Negulescu, namely Axel Maupoux and Etienne Lehman. Furthermore the numerical plots were also furnished by these PhD students, such that their contribution was very useful for rendering this work comprehensible and beneficial. The PhD of Axel Maupoux is financed by the French Defence Innovation Agency, whereas Etienne Lehman is financed by the Ecole Normale Supérieure de Lyon.

Contents

Introduction	3
0.1 Collective behaviour in nature	4
0.2 Drones	5
0.3 Mathematical problematic	6
0.3.1 ODE, Lyapunov functional, equilibrium	6
0.4 Some examples of flocking models	9
0.4.1 Cucker-Smale model	10
0.4.2 Three-zone model	12
0.4.3 Other collective behaviour models	13
0.5 Different levels of mathematical description	14
1 The Fokker-Planck equation	17
1.1 The Langevin system	17
1.2 The Fokker-Planck equation	19
1.3 Properties and remarks	21
1.4 Variational framework for the Fokker-Planck equation	23
2 Entropy methods	27
2.1 Coercivity versus Hypo-coercivity	30
2.2 Two simple, linear algebraic examples	33
2.3 The heat equation (coercive case)	34
2.4 Fokker-Planck equation	37
2.4.1 The homogeneous Fokker-Planck equation (coercive case)	37
2.4.2 The inhomogeneous Fokker-Planck equation (hypocoercive case)	38
2.5 The three-zone model (hypocoercive case)	40
3 Drone swarm modelling and simulation	45
3.1 Some equilibrium configurations	46
3.2 Specificities of drone swarms and other physical effects	49
3.3 Mesoscopic and macroscopic descriptions	51
3.3.1 Kinetic descriptions	52
3.3.2 Fluid descriptions	55
3.3.3 Long-time asymptotics	56

4	Some fundamental inequalities	61
4.1	Gronwall lemma	61
4.2	Poincaré inequality	62
4.3	Logarithmic Sobolev inequalities	63
4.4	Csiszár-Kullback inequality	64
	Summary	65
	Bibliographie	67

Introduction

The central theme of this course is the introduction of a mathematical model for the description of an autonomous drone swarm, constituted of a large number of drones which shall self-organize and cooperate in order to perform collective tasks in real-world situations, such as assistance in emergency situations (forest fire, avalanche, shipwreck, earthquake, *etc*), oil and gas pipelines surveys, geo-magnetic surveys, protection of vulnerable sites *etc*. The model will be based on simple mathematical rules describing the inter-drone interaction forces, like repulsion and attraction for example and resulting in a global behaviour of the whole swarm. A detailed mathematical analysis of the designed model as well as numerical simulations shall be performed with the aim to remain as close as possible to reality.

Understanding the essential characteristics of the emergent collective behaviour of a drone swarm, requires a deep understanding of the repercussion of each (inter-drone) force on the overall collective behaviour, as well as of the influence of several factors, such as the environment, time-delays in the reaction times and inertial effects of the drones as well as inaccuracies of the on-board sensors. Thus a lot of aspects enter into the modelling, rendering the design of such autonomous drone swarms very challenging and interesting from a mathematical point of view.

The present work is thus concerned with the mathematical modelling and analysis of the autonomous dynamics of a drone swarm. Numerical simulations will be also performed. The manuscript is composed of the following chapters:

- The introduction gives a general overview of the existing theory in this domain;
- Chapter 1 explains briefly how to obtain the Fokker-Planck equation from the underlying Langevin's system, which corresponds to Newton's laws with an additional stochastic force field (noise term); this part is necessary to understand the mesoscopic description of particle swarms;
- Chapter 2 introduces the entropy methods as a “standard” mathematical tool for the investigation of the long-time behaviour of solutions to ODE systems;
- Chapter 3 is the main part of this course and deals with the particular case of drone swarm modelling and the mathematical as well as numerical analysis of the proposed model;
- Chapter 4 regroups some fundamental lemmas and inequalities necessary in the whole manuscript.

0.1 Collective behaviour in nature

Collective motion or self-organization is an astonishing phenomenon, that can be observed in various natural processes, such as fish schools, bird flocks, herds of bulls or sheep, insect swarms, cellular dynamics, pedestrian behaviours *etc* (see Fig. 1). Patterns appear due to the organized (cooperative) motion of a large number of small constituents. Such natural systems composed of inter-connected particles tend to self-organize into macroscopic structures with the aim to form more intelligent or more adaptive large-scale dynamics. Self-organization does not happen by chance, but rather due to the numerous, specific interactions among the lower-level components of the system. The rules specifying these interactions among the components are local, without reference to the global behaviour of the swarm, and decisions are made by the components/particle themselves.



Figure 1: Examples of collective behaviours arising in nature [41–43].

The underlying forces leading to self-organization can be of various type, as for example:

- physical mechanisms (gravity, electromagnetic forces, nuclear forces, ...);
- chemical mechanisms (pheromones, Van-der-Waals forces, ...);
- instinctive survival mechanisms (fear, feeding, ...).

Self-organized systems obey evolution equations which are generally highly non-linear. Such models take the form of ODE systems or transport-type PDEs, where the individuals are submitted to forces generated by their neighbours. Depending on the nature of the inter-particle interactions, the collective behaviour of the swarm may differ, for instance individuals can aggregate, align their velocities or disperse.

The systematic mathematical study of "flocking"-models began with Viscek and his collaborators [?], with the introduction of a stochastic, time-discrete model. Later Cucker-Smale [18, 19] proposed a deterministic, time-continuous model. Other models have been then proposed for the description of the collective fish behaviour [21, 36] and bacteria [11]. Among the numerous existing models one is particularly appreciated, namely the three-zone model, based on Reynold's empirical rules, namely

- **Flocking:** the desire of individuals to stay together, for safety or social reasons;
- **Collision avoidance:** individuals tend to repel, when coming too close together;
- **Velocity matching:** attempt to keep similar velocities and flying directions as its neighbours.

0.2 Drones

To model mathematically the dynamics of a swarm of autonomous flying robots like drones, the observation of natural emergent systems can offer lot of inspiration. By autonomous we mean that every agent uses on-board sensors to measure its state as well as the states of its neighbours and performs all controlling computations with an on-board computer, i.e. the control system is decentralized (see Fig. 2 for some ex.). Important to underline is that the paths of the agents are not predefined, but emergent from the underlying inter-particle relations as well as from exterior force-fields.

One essential question to be asked is: "Which is the interaction between the individuals at the microscopic level, which gives rise to the desired macroscopic behaviour?" There is no need to assume sophisticated local inter-particle connections to provoke a complex macroscopic pattern. Models describing clouds or swarms of particles are essentially based on a delicate balance between long-range attraction (to form a cloud) and short-range repulsion (to avoid collisions). Only when the desired macroscopic dynamics is not obtained, more complex rules have to be considered. Contrary to existing models for biological swarm behaviours, in a drone model one should additionally take into account some system-specific features, such as:

- **Inertia:** The drones are unable to change immediately their position and velocity, due to their inherent inertia;
- **Time delays:** Each drone needs time to receive and process the information got from its neighbours;
- **Noise:** Inaccuracy of the sensors measuring the position and velocity of the drone itself as well as of its neighbours is a so-called "inner noise" to be taken into account, whereas "outer noise" are unpredictable environmental effects, such as the wind for example;
- **Autonomy:** Small batteries due to weight restrictions lead to short life-times for drones.

Other aspects which have to be taken into account, are for example the fact that losing one or more drones has to have little impact on the overall swarm dynamics. Without going too much into details, it is clear that an engineer has also other criteria to consider, as flexibility and robustness of the drone swarm, efficiency and cost constraints.

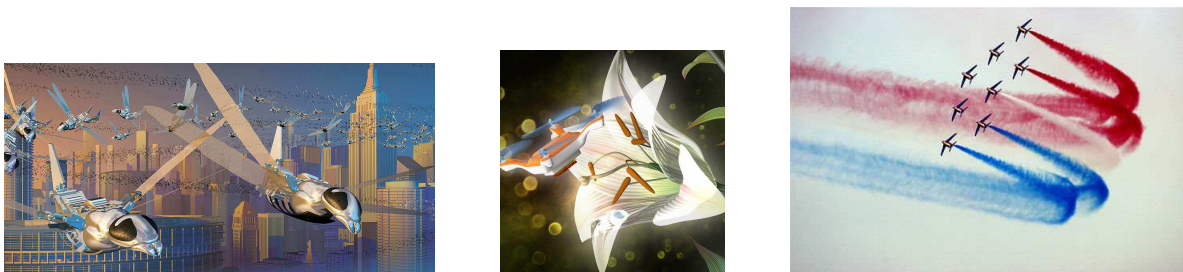


Figure 2: Examples of application of some drone swarms [44–46].

0.3 Mathematical problematic

Modelling is the art of taking a real-world situation and of trying to find an accurate mathematical description for it. It is more than a science, because it involves choices that can not really/rationally be justified. Intuition and personal preferences for example play a major role (for ex. when deciding whether a deterministic or a stochastic approach is better adapted for a specific situation). To imagine how difficult such mathematical modelling can be in our particular situation, think of some questions which might be asked, like “*Why do we choose this type of a repulsion/attraction force between drones?*” or “*Why does one model the environment in such a manner?*” Furthermore, a mathematical model should not only reproduce a specific natural phenomenon, but it has also to be consistent with this phenomenon, meaning that the chosen parameters, as for ex. the maximal velocity of the agents, have to be conceivable from a physical/natural point of view.

At the microscopic level, the dynamics of a cloud composed of N particles is based on Newton’s classical laws of mechanics, describing the time-evolution of the position of each individual $x_i(t)$ as well as of its velocity $v_i(t)$ via the equation

$$\begin{cases} x'_i(t) = v_i(t), \\ v'_i(t) = F^{ext}(t, x_i, v_i) + F_i^{int}(x_1, \dots, x_N, v_1, \dots, v_N), \end{cases} \quad \forall i = 1, \dots, N, \quad (1)$$

where F^{ext} represents an exterior force term, for example describing the wind, obstacles or the target of the drones, and F_i^{int} is the inter-particle force term exerted on particle i by the other surrounding particles. We are thus concerned with a coupled, non-linear ODE system, which cannot be solved explicitly, however some qualitative study of the stability of particular solutions, such as equilibrium patterns, can be performed as well as the study of long-time asymptotic.

The delicate modelling part is now to choose adequate force terms, which permit a realistic description of the collective behaviour one is observing or is interested to generate. Depending on the specific choice of these force terms the model can have rather different properties. The inter-drone interaction force is directly responsible for the emergence of specific patterns, like milling, flocking, clustering, *etc.*

0.3.1 ODE, Lyapunov functional, equilibrium

As we just saw, the mathematical modelling of collective behaviours in nature leads to ODE systems of the following form

$$\begin{cases} u'(t) = f(t, u(t)), & \forall t > 0, \\ u(0) = u_0 \in \Omega, \end{cases} \quad (2)$$

where the (non-linear) function $f : \mathbb{R}_0^+ \times \Omega \rightarrow \mathbb{R}^d$, with $\Omega \subset \mathbb{R}^d$, is assumed to satisfy the standard conditions for the existence and uniqueness of a global solution $u : \mathbb{R}_0^+ \rightarrow \Omega$ (Cauchy-Lipschitz theorem). Let us recall now rapidly the mathematical tools of Lyapunov stability theory, permitting to analyse in more details the long-time behaviour of such ODEs.

Definition 0.3.1 (Equilibrium point)

A solution u^* is called equilibrium corresponding to (2) if $f(t, u^*) \equiv 0$ for all $t \geq 0$.

Remark that by translation one assumes often that the investigated equilibrium point is $u^* \equiv 0$. Moreover, if several equilibria exist, one usually investigates the stability of each one separately.

Definition 0.3.2 (Stability in the sense of Lyapunov)

The equilibrium point u^* is stable in the sense of Lyapunov if for each $\varepsilon > 0$ there exists a constant $\delta > 0$ such that one has the implication

$$\|u(0) - u^*\| < \delta \quad \Rightarrow \quad \|u(t) - u^*\| < \varepsilon \quad \forall t > 0.$$

An equilibrium point is said to be "unstable", if it is not stable.

Lyapunov stability is a very mild requirement for equilibrium points, as it does not require that trajectories starting near an equilibrium, tend towards this equilibrium asymptotically in time, *i.e.* for $t \rightarrow \infty$.

Definition 0.3.3 (Asymptotic stability)

The equilibrium u^* of (2) is asymptotically stable, if

- u^* is stable (in the sense of Lyapunov);
- u^* is locally attractive, meaning there exists $\delta > 0$ such that

$$\|u(0) - u^*\| < \delta \quad \Rightarrow \quad \lim_{t \rightarrow \infty} u(t) = u^*.$$

It is important to note that the definition of asymptotic stability does not quantify the rate of convergence towards this equilibrium.

Definition 0.3.4 (Exponential stability)

The equilibrium u^* of (2) is exponentially stable if there exist some constants $C, \kappa > 0$ and $\delta > 0$ such that

$$\|u(0) - u^*\| < \delta \quad \Rightarrow \quad \|u(t) - u^*\| \leq C e^{-\kappa t} \|u_0 - u^*\|, \quad \forall t > 0.$$

The largest constant $\kappa > 0$ which may be used is called "rate of convergence".

Exponential stability is a strong form of stability, which is very useful in applications. Indeed, exponentially stable equilibria are very robust with respect to perturbations and are hence preferred configurations.

Very often it is possible to determine whether an equilibrium of a nonlinear system is locally stable, by simply investigating the stability of the corresponding linearized system, linearized around the equilibrium point. This approach is the so-called **Lyapunov's linearized method**, and is based on the following theorem.

Let us consider the following linearized system, with $A \in \mathbb{R}^{d \times d}$ a constant matrix and $u_0 \in \mathbb{R}^d$

$$\begin{cases} u'(t) = A u(t), & \forall t > 0, \\ u(0) = u_0. \end{cases} \quad (3)$$

Lemma 0.3.5 (Stability of linear systems)

Let us assume that A is regular, such that $u^* \equiv 0$ is the only equilibrium of (3). If

- A has at least one eigenvalue with strictly positive real part, then the equilibrium u^* is unstable;
- A has all eigenvalues with non-positive real parts, and those eigenvalues having zero real-part are non-defective (algebraic multiplicity is equal to geometric one), then the equilibrium u^* is stable;
- A has all eigenvalues with negative real parts, then the equilibrium u^* is asymptotically stable.

Lyapunov's direct method is different and allows to determine the stability of a system without linearization and without explicitly integrating the differential equation. The method is based on some physical arguments, in particular on the existence of some “energy” or “entropy” \mathcal{E} in the system and on the study of the rate of change of this energy during the time evolution of the system. Briefly, if \mathcal{E} is positive definite and its derivative along the trajectories $u(t)$ of the system is non-positive, then one can show that the equilibrium point is stable. By imposing additional conditions on \mathcal{E} and $\frac{d}{dt}\mathcal{E}(u(t))$ one can even show asymptotical or exponential stability, both locally and globally.

To be more precise, let us consider the autonomous system

$$\begin{cases} u'(t) = f(u(t)), & \forall t > 0, \\ u(0) = u_0 \in \Omega, \end{cases} \quad (4)$$

with $f : \Omega \subset \mathbb{R}^d \rightarrow \mathbb{R}^d$ being of class C^1 (could be rendered weaker), assuming that a global solution $u : \mathbb{R}_0^+ \rightarrow \Omega$ exists, and let $u^* \in \Omega$ be the unique equilibrium solution.

Definition 0.3.6 (Positive definite function)

A continuous function $\mathcal{E} : \Omega \subset \mathbb{R}^d \rightarrow \mathbb{R}$, satisfying

$$\mathcal{E}(u) > 0, \quad \forall u \in \Omega \setminus \{u^*\}, \quad \text{as well as} \quad \mathcal{E}(u^*) = 0,$$

is called *positive definite (around u^*)*. If these requirements are valid only locally, meaning for all $u \in \Omega$ with $\|u - u^*\| \leq R$, then one says that \mathcal{E} is *locally positive definite*.

Theorem 0.3.7 (Stability/asymptotic stability)

Let us consider the autonomous ODE (4), with solution $u : \mathbb{R}_0^+ \rightarrow \Omega$ and equilibrium point $u^* \in \Omega$. If there exists a continuously differentiable functional $\mathcal{E} : \Omega \subset \mathbb{R}^d \rightarrow \mathbb{R}$, such that

- (i) \mathcal{E} is positive definite around u^* and
 - (ii) $\frac{d}{dt}\mathcal{E}(u(t)) \leq 0$ along all trajectories $u(t)$ of (4),
- then the equilibrium u^* is stable.

If in addition

- (iii) $-\frac{d}{dt}\mathcal{E}(u(t))$ is positive definite around u^* ,
- then u^* is asymptotically stable.

Exponential stability is a special case of asymptotic stability, with a particular convergence rate.

Theorem 0.3.8 (Exponential stability)

Let us consider the autonomous ODE (4), with solution $u : \mathbb{R}_0^+ \rightarrow \Omega$ and equilibrium point $u^* \in \Omega$. If there exists a continuously differentiable functional $\mathcal{E} : \Omega \subset \mathbb{R}^d \rightarrow \mathbb{R}$, such that

- (i) \mathcal{E} is positive definite around u^* and
- (ii) $\frac{d}{dt}\mathcal{E}(u(t)) \leq -\kappa \mathcal{E}(u(t))$ along all trajectories of (4), with some constant $\kappa > 0$, then u^* is exponentially stable.

In Chapter 2 we shall give some details about how to find such Lyapunov functionals for specific ODE-systems and how to prove the asymptotic stability of equilibrium solutions.

0.4 Some examples of flocking models

Let us consider in the following a particle system consisting of N identical agents with positions and velocities denoted by $(x_i(t), v_i(t)) \in \mathbb{R}^d \times \mathbb{R}^d$, and masses $m_i = 1$ for $i = 1, \dots, N$, where $d = 2$ or $d = 3$. The particles are interacting with each other via simple local rules, to be defined in the following. The aim is to investigate, starting from a given initial configuration $(x_i^0, v_i^0)_{i=1}^N \in (\mathbb{R}^d \times \mathbb{R}^d)^N$, the long time behaviour of the whole particle system. For this, let us define what we mean with **flocking**.

Definition 0.4.1 A multi-particle system $\{(x_i, v_i)\}_{i=1}^N$ is said to have an asymptotic flocking pattern, if the following two conditions are satisfied:

- (i) **(Aggregation)** The spatial diameter $\mathcal{D}(t)$ of the particle cloud is uniformly bounded in time, meaning

$$\sup_{t \geq 0} \mathcal{D}(t) < \infty, \quad \mathcal{D}(t) := \max_{i,j} |x_i(t) - x_j(t)|.$$

- (ii) **(Velocity alignment)** The velocity diameter $\mathcal{A}(t)$ of the particle cloud tends towards zero as $t \rightarrow \infty$, namely

$$\lim_{t \rightarrow \infty} \mathcal{A}(t) = 0, \quad \mathcal{A}(t) := \max_{i,j} |v_i(t) - v_j(t)|.$$

Flocking requires thus the emergence of alignment, hence consensus in velocity. Often the word *swarming* appears also in literature, usually in relation with insect swarms. It is a less restrictive notion than *flocking*, requiring only cohesion, namely

$$\sup_{t \geq 0} \max_i |x_i(t) - x_c(t)| < \infty, \quad \sup_{t \geq 0} \max_i |v_i(t) - v_c(t)| < \infty,$$

where

$$x_c(t) := \frac{1}{N} \sum_{i=1}^N x_i(t), \quad v_c(t) := \frac{1}{N} \sum_{i=1}^N v_i(t), \quad \forall t \in \mathbb{R}^+,$$

are the average position and velocity of the particle cloud. Let us present now two well-known mathematical models for the description of a particle flock dynamics and recall the results permitting to show flocking under certain conditions.

0.4.1 Cucker-Smale model

The Cucker-Smale model is a very basic model describing the dynamics of a cloud consisting of N particles submitted only to a velocity-alignment force, permitting to obtain a certain self-organization (flocking), if the communication function is sufficiently large as shall be seen in the following. The evolution of each particle, with position and velocity $(x_i, v_i) \in \mathbb{R}^d \times \mathbb{R}^d$ is governed for all $t \geq 0$ by Newton's laws

$$\begin{cases} x_i'(t) = v_i(t), \\ v_i'(t) = \frac{1}{N} \sum_{j=1}^N \psi(|x_i - x_j|) (v_j - v_i), \end{cases} \quad \forall i = 1, \dots, N, \quad (5)$$

where $\psi_{ij} := \psi(|x_i - x_j|)$ represents the strength of the velocity-alignment (*communication strength*) between individual i and j and depends on the relative distance between the particles. One often assumes that ψ is a positive, decreasing function, *i.e.* satisfying

$$\psi \in C^1(\mathbb{R}_*^+), \quad \psi(r) > 0 \quad \text{and} \quad \psi'(r) \leq 0 \quad \forall r > 0. \quad (6)$$

Two simple communication strengths can be found in literature, a bounded respectively a singular one, namely

$$\psi_b(r) := \frac{\alpha}{(1+r^2)^{\beta/2}}, \quad \psi_s(r) := \frac{\alpha}{r^\beta}, \quad \alpha > 0, \beta \geq 0, r \in \mathbb{R}^+. \quad (7)$$

The strength of the communication weight is often expressed in terms of integrability conditions at short or long range, such as (for some fixed $r_0 > 0$)

$$\begin{aligned} \int_{r_0}^{\infty} \psi(r) dr &= \infty && \text{(long range condition, heavy tail),} \\ \int_0^{r_0} \psi(r) dr &= \infty && \text{(short range condition).} \end{aligned}$$

These conditions guarantee unconditional flocking and collision avoidance respectively and are not necessary conditions (see Theorems 0.4.2 and 0.4.3). Let us observe furthermore that the symmetry of the communication weight ($\psi_{ij} = \psi_{ji}$) implies immediately the conservation of the total momentum. Indeed, introducing the center of mass couple $(x_c(t), v_c(t))$ via

$$x_c(t) := \frac{1}{N} \sum_{i=1}^N x_i(t), \quad v_c(t) := \frac{1}{N} \sum_{i=1}^N v_i(t), \quad \forall t \in \mathbb{R}^+,$$

one can show that $v_c(t) = v_c(0)$ and $x_c(t) = x_c(0) + tv_c(0)$, such that by translation, one can assume in the following that

$$x_c(t) \equiv 0, \quad v_c(t) \equiv 0, \quad \forall t \in \mathbb{R}^+.$$

Let us introduce furthermore the notation

$$X(t) := (x_i(t))_{i=1}^N, \quad \|X\|_2^2 := \sum_{i=1}^N |x_i|^2, \quad \|X\|_\infty := \max_{1 \leq i \leq N} |x_i|.$$

Then one has the following flocking theorem in the regular case:

Theorem 0.4.2 [30] **(Flocking in the bounded case)**

Let $(x_i, v_i)_{i=1}^N$ be the unique global solution to (5) with regular communication weight ψ_b and initial conditions which are non-collisional, namely $x_i^0 \neq x_j^0$ for all $1 \leq i \neq j \leq N$. Then :

(i) if $\beta \in [0, 1]$ (long-range cond.), one has an **unconditional flocking**, meaning there exist two constants d_m, d_M such that

$$0 \leq d_m \leq \|X(t)\|_2 \leq d_M, \quad \|V(t)\|_2 \leq \|V^0\|_2 e^{-\psi_b(d_M)t}, \quad \forall t \in \mathbb{R}^+.$$

(ii) if $\beta \in (1, \infty)$, we are in the **conditional flocking** case, namely for initial conditions satisfying $\|V^0\|_2 < \int_{\|X^0\|_2}^{\infty} \psi_b(r) dr$, there exist two constants d_m, d_M such that

$$0 \leq d_m \leq \|X(t)\|_2 \leq d_M, \quad \|V(t)\|_2 \leq \|V^0\|_2 e^{-\psi_b(d_M)t}, \quad \forall t \in \mathbb{R}^+.$$

(iii) for any $\beta \geq 0$ if one has additionally $\|V^0\|_2 < \int_0^{\|X^0\|_2} \psi_b(r) dr$, then $d_m > 0$.

In the bounded case, the long-range condition (i) guarantees unconditional flocking for the Cucker-Smale model, regardless the initial condition. If not, one can still ensure flocking, however assuming an initial restriction on the velocity V^0 (condition (ii)). This last theorem does after all not say anything about the fact whether the particles collide or not, it only tells us that no finite-time collapse to a one-point configuration can occur if $d_m > 0$.

In the strong singular case ($\beta \geq 1$), one can show more, namely the absence of collisions between agents, regardless the initial data. Let us denote the distance between the particles as $r_{ij}(t) := |x_i(t) - x_j(t)|$, then we have the following result.

Theorem 0.4.3 [16] **(Flocking in the singular case)**

Let us consider (5) with singular communication weight ψ_s satisfying (6) as well as the strong singularity condition in $r = 0$ (short-range cond.), i.e.

$$\int_0^{r_0} \psi_s(r) dr = \infty \quad \text{for each } r_0 > 0,$$

which is for ex. satisfied for $\psi_s(r) = \frac{\alpha}{r^\beta}$ with $\alpha > 0$ and $\beta \geq 1$ and assume initial conditions which are non-collisional, namely $x_i^0 \neq x_j^0$ for all $1 \leq i \neq j \leq N$. Then

(i) system (5) admits a unique global and smooth solution in time, with non-collisional trajectories, namely

$$x_i(t) \neq x_j(t) \quad \text{for all } 1 \leq i \neq j \leq N \quad \text{and } \forall t \geq 0;$$

(ii) if furthermore the initial conditions satisfy the condition

$$\|V^0\|_\infty < \frac{1}{2} \int_{2\|X^0\|_\infty}^{\infty} \psi_s(r) dr,$$

there exist positive functions resp. constants $0 < r_m(t) < r_M$ such that

$$0 < r_m(t) \leq r_{ij}(t) \leq r_M, \quad \|V(t)\|_\infty \leq \|V^0\|_\infty e^{-\psi_s(2r_M)t}, \quad \forall t \in \mathbb{R}^+.$$

Note that $r_m(t)$ might go to zero as $t \rightarrow \infty$, such that collisions are possible in the asymptotics of long time.

In the weak singularity case ($\beta \in (0, 1)$) the particles can collide and stick together, the existence of a unique (local) solution is however obtained thanks to the weak singularity of ψ_s , in particular to the integrability of ψ_s at the origin [37, 38].

0.4.2 Three-zone model

The three-zone model describes the dynamics of the cloud of N particles via three simple interaction rules, namely repulsion at short-range, alignment and attraction at long-range. The evolution of each particle, with position and velocity $(x_i, v_i) \in \mathbb{R}^d \times \mathbb{R}^d$, is governed by the following Newton's laws

$$\begin{cases} x_i'(t) = v_i(t), \\ v_i'(t) = \frac{1}{N} \sum_{j=1}^N \psi(|x_i - x_j|) (v_j - v_i) - \frac{1}{N} \sum_{j=1, j \neq i}^N \nabla_{x_i} [\varphi(|x_i - x_j|)], \end{cases} \quad \forall i = 1, \dots, N, \quad (8)$$

where the function $\psi_{ij} := \psi(|x_i - x_j|)$ is the communication weight between the particles, satisfying the assumptions of the Cucker-Smale model for example. Concerning the potential φ it contains the repulsion and attraction part, and we shall assume that

$$\varphi \in C^1(\mathbb{R}_*^+), \quad \varphi(r) > 0 \quad \forall r > 0, \quad \lim_{r \rightarrow 0, \infty} \varphi(r) = \infty. \quad (9)$$

Remark that

$$\nabla_{x_i} \varphi(r_{ij}) = -\varphi'(r_{ij}) \frac{x_j - x_i}{r_{ij}}, \quad r_{ij}(t) := |x_i(t) - x_j(t)|,$$

such that we have attraction for $\varphi'(r) > 0$ and repulsion in the contrary case (see Fig. 3).

Remark 0.4.4 *Condition (9) is used in these lectures to simplify the proofs, however it can be weakend, as one can observe on the figures we draw and in the numerical simulations we shall present later. Indeed, for having a bounded swarm, one finally only needs a smooth potential φ under the form of a potential well, however providing then extra hypothesis on the initial energy of the particles, in order for them not to escape from the well.*

Theorem 0.4.5 [12] (Flocking for the 3-zone model)

Let us suppose the communication weight ψ_b is bounded, and ψ_b resp. φ are satisfying (6) resp. (9). Then for any non-collisional initial condition $(x_i^0, v_i^0)_{i=1}^N$ the three zone model (8) admits a unique global solution $(x_i, v_i)_{i=1}^N$, which converges asymptotically in time towards a flock, meaning there exist two constants $r_m, r_M > 0$ (dependent on N but not on t), such that for all $i, j = 1, \dots, N$

$$0 < r_m \leq r_{ij}(t) \leq r_M \quad \forall t \geq 0, \quad \mathcal{A}(t) \rightarrow_{t \rightarrow \infty} 0.$$

In particular no collisions occur during the dynamics of the system.

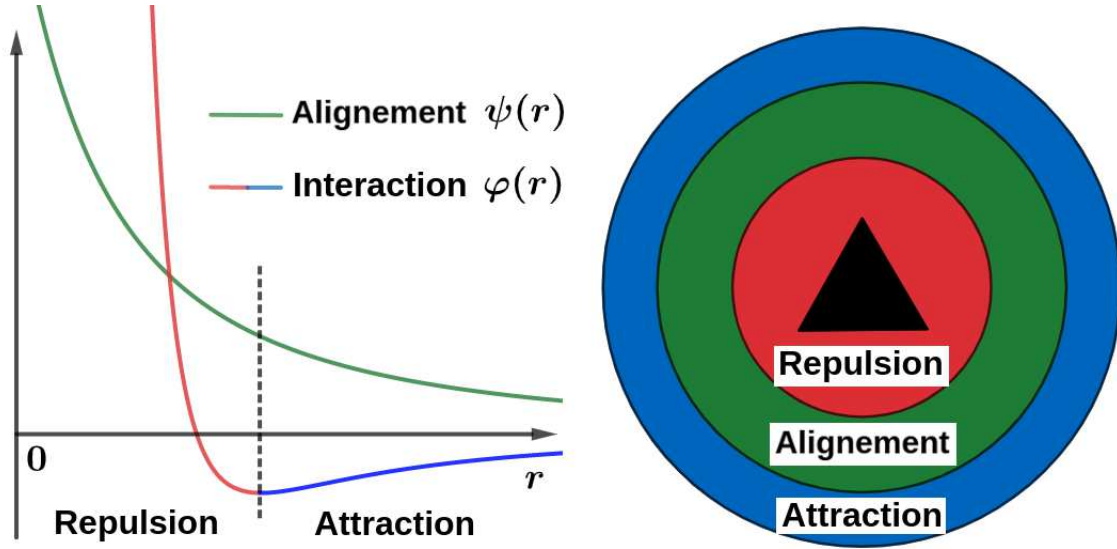


Figure 3: Illustration of the three zone model interaction potentials.

0.4.3 Other collective behaviour models

These lectures are not intended to cover the whole range of models proposed in literature for self-organized systems. Our work concerns most specifically the modelling of drone swarms, such that we shall focus on the Cucker-Smale and the three zone model presented above. However, for completeness reasons, let us mention in this subsection briefly some words about other well-known models. All these models offer a number of mathematically interesting properties, such as flocking behaviour, (exponential) convergence towards equilibrium states, phase-transitions *etc*, we refer the interested reader to take a look at the papers cited below, for the mathematical results. A nice review is given in [14].

Continuous Vicsek model [22, 39]. A simple model widely used in literature to describe the dynamics of N point-like, self-propelled particles, evolving with a constant speed $c > 0$, is given by the following continuous Vicsek model

$$\begin{cases} x'_i(t) = c \omega_i(t), \\ \omega'_i(t) = (\mathbb{I}_d - \omega_i \otimes \omega_i) \bar{\omega}_i, \end{cases} \quad \forall i = 1, \dots, N, \quad (10)$$

where $x_i(t) \in \mathbb{R}^d$ and $\omega_i(t) \in \mathbb{S}^{d-1}$ are the positions respectively the orientations of the particles and where

$$\bar{\omega}_i(t) := \frac{J_i(t)}{|J_i(t)|}, \quad J_i(t) := \sum_{j, |x_i - x_j| \leq R} \omega_j(t),$$

with $R > 0$ being the interaction range of the particles. The Vicsek model has been proposed to describe the interactions among animal groups, such as fish schools. The individuals move with a constant velocity, their orientation being continuously (or discretely) updated by the direction of the average velocities of the neighbouring individuals

(sometimes with additional noise terms). The matrix $(\mathbb{I}_d - \omega_i \otimes \omega_i)$ corresponds to the orthogonal projector on ω_i^\perp . Its role is to ensure that the orientation ω_i remains at all times in \mathbb{S}^{d-1} . Remark that this model considers only alignment without attraction and/or repulsion. It permits also to investigate phase-transitions between ordered and disordered states, whenever the noise strength or the particle number is varied. The link between the Vicsek model and the Cucker-Smale model is investigated in [8].

Kuramoto model [34, 35]. This model is an archetype model for synchronisation behaviour in heterogeneous systems of coupled oscillators, introduced to model the collective dynamics of biological and neural oscillator networks. The model describes the dynamics of N coupled oscillators with natural frequencies $\omega_i(t)$, via the evolution of the phase function $\vartheta_i(t)$, solution of the coupled ODE system

$$\vartheta_i'(t) = \omega_i + \frac{K}{N} \sum_{j=1}^N \sin(\vartheta_j(t) - \vartheta_i(t)), \quad \forall i = 1, \dots, N, \quad (11)$$

where $K > 0$ is the coupling strength between the oscillators. Individuals are hence influenced at the microscopic level through pairwise attractive interactions, leading to an overall collective movement, such as the emergence of synchronisation when all individuals oscillate in union. Synchrony seems to be essential to the proper functioning of life processes, such that this model is intensively used to describe several spontaneous synchronisation phenomena in cardiac or nervous systems.

Aggregation models [17, 33]. At cellular scale, the collective migration of cohesive cell groups and their aggregation sets up the basis of the formation of complex tissues (vascular and neural structures, cancer growth *etc*). A proper description of the intercellular pairwise interactions is a challenging task, the pattern formation being a combination of adhesive and repulsive mechanisms. Cells have also the particularity to move in extremely viscous environments, such that inertial terms can be neglected and first order models are usually employed, *i.e.*

$$\lambda_i x_i'(t) = F_i(t), \quad F_i(t) = - \sum_{j=1}^N K(|x_i(t) - x_j(t)|) \frac{x_i(t) - x_j(t)}{|x_i(t) - x_j(t)|}, \quad \forall i = 1, \dots, N,$$

where $\lambda_i > 0$ are the cell-substrate friction coefficients and F_i is the force acting on cell i , given for example via a well chosen interaction kernel K .

0.5 Different levels of mathematical description

Let us finish this introductory chapter by remarking that many choices have to be made in order to work out a mathematical model for the description of a specific phenomenon. For example one has to single out if a deterministic or a stochastic model is better suited for the description, or to decide whether a discrete or a continuous approach is more adequate. Furthermore in the context of the dynamics of large systems of interacting particles, the level of description has also its importance, in particular one can distinguish between:

- the **particle description**, based on the laws of motion of classical mechanics (Newton's laws) for the description of each individual particle trajectory $(x_i(t), v_i(t))_{i=1}^N$ (individual-based models);
→ the particle dynamic model is the most intuitive and physically most accurate one, but also the most inadequate/heavy from a numerical point of view ($6N$ degrees of freedom, where N is the number of particles).
- the **kinetic description**, based on a collective swarm description via the particle distribution function $f(t, x, v)$, solution of the Vlasov equation. Here $f(t, x, v) dv dx$ represents the number of particles to be found at time t in the infinitesimal phase-space volume $dv dx$ around (x, v) ;
→ although the precise locations of the individual particles are lost in the kinetic theory, sufficient knowledge of the particle motion is still incorporated and the numerical costs are still rather high, the system being 6 dimensional.
- the **fluid description**, describing the particle swarm in terms of averaged macroscopic quantities, depending only on t and x , as for example the particle density $n(t, x)$, the velocity $u(t, x)$, the pressure $p(t, x)$, solutions of the well-known conservation laws of fluid mechanics;
→ fluid models are numerically very attractive, but poor from a physical point of view, based on some empirical assumptions for the closure.

These successive models differ in complexity and precision. They are increasingly simplified, in the sense that they can be obtained from one another by decreasing the number of degrees of freedom, hereby becoming less accurate. Depending on the physical phenomenon one wants to investigate, one has to choose within all these models the one which is the most accurate with respect to the particular physical situation, paying attention at the same time to the numerical costs.

Finally, let us also mention that when designing a collective dynamics model, the mathematical description of the inter-particle interactions is not a simple task. It strongly depends on the specific nature of the examined population, for example if one considers animals, humans or robots. The different internal (microscopic) behaviours of these three populations can then be observed on the emergent (macroscopic) overall behaviour. For example humans are much more individualists than animals, thus it is more difficult for humans to be part of a group and this originality has to be taken into account in the inter-particle description. For animals hierarchy and rules are very important. A real population is a complex system, it involves plenty of physical, social, biological and cognitive variables. Contrary to animals and humans, robots (drones for ex.) are designed, such that the inter-particle rules are often imagined by the designer and not given by a natural law. However these rules have to be realistic from a practical point of view.

Chapter 1

The Fokker-Planck equation

In this chapter we shall explain how one obtains the Fokker-Planck equation starting from Newton's laws of classical mechanics, where some stochastic noise has been introduced, to describe the interaction with an environment. The concept of "stochastic process" is needed for this.

This chapter could seem somehow apart in this manuscript, however it shows how one makes the link between the microscopic models (for ex. the individual-based models) and the mesoscopic models, namely the kinetic approach.

1.1 The Langevin system

The botanist Robert Brown (1773-1858) investigated the chaotic movement of pollen-particles in suspension in water. At that time the scientific world was influenced by Newton's mechanics and its determinism, such that the erratic dynamics of the pollen-particles generated rather hard interpretation problems.

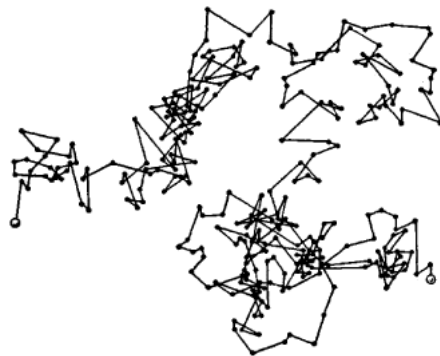


Figure 1.1: Example of the erratic dynamics of a particle.

The main idea of Paul Langevin (1872-1946) was that *Newton's equations* of classical mechanics remain valid in average for the Brownian, erratic particle motion. Thus, for a particle evolving in a viscous environment with friction coefficient $\gamma > 0$, the average dynamics is given by Newton's laws

$$m \frac{d}{dt} \langle v(t) \rangle = -m\gamma \langle v(t) \rangle, \quad \text{where} \quad \langle v(t) \rangle = \frac{d}{dt} \langle x(t) \rangle, \quad \forall t \in \mathbb{R}.$$

The average $\langle \cdot \rangle$ is taken over all possible trajectories of the particles submitted to a random force field $\eta(t)$. The equation however which governs in detail the dynamics of one particle submitted to this force field $\eta(t)$ (noise term) is the so-called *Langevin equation* given by

$$\frac{d}{dt} v(t) = -\gamma v(t) + \eta(t), \quad \forall t \in \mathbb{R}. \quad (1.1)$$

It is a stochastic differential equation, which incorporates two force terms, the viscous force $-\gamma v(t)$ and a fluctuating force $\eta(t)$, which represents the incessant impacts of the environmental molecules on our Brownian particle. The choice of this last force field $\eta(t)$ is done in such a manner to model in the most realistic way the effects of the microscopic collisions on the particles. It is an unknown force field, rather complicated, and which has to be treated stochastically. We shall suppose that $\eta(t)$ has a Gaussian distribution (Gaussian white noise), meaning that we assume zero average and zero correlation time, *i.e.*

$$\langle \eta(t) \rangle = 0, \quad \langle \eta(t) \eta(t') \rangle = \Gamma \delta_0(t - t'), \quad \Gamma > 0, \quad \forall t, t' > 0. \quad (1.2)$$

The constant $\Gamma > 0$ measures somehow the strength of the fluctuating force-field. Each solution of the Langevin equation (1.1) represents a different trajectory of the particle, depending on the initial condition v_0 as well as on the random force field $\eta(t)$, and is given by Duhamel's formula

$$v(t) = v_0 e^{-\gamma t} + \int_0^t e^{-\gamma(t-s)} \eta(s) ds, \quad \forall t > 0. \quad (1.3)$$

As $\eta(t)$ is a Gaussian stochastic process and as the sum or the integral of Gaussian variables are again Gaussian variables, we can deduce that $v(t)$ is also a Gaussian stochastic process. Hence for its characterization it is enough to compute the average $\mu(t) = \langle v(t) \rangle$ and the variance $\sigma(t)$, averaging over all possible outputs, and to define the corresponding velocity probability distribution function via

$$f(t, v) := \frac{1}{\sqrt{2\pi\sigma^2(t)}} e^{-\frac{(v-\mu(t))^2}{2\sigma^2(t)}}. \quad (1.4)$$

In view of properties (1.2), we get by averaging (1.3) on one hand

$$\langle v(t) \rangle = v_0 e^{-\gamma t} \xrightarrow{t \rightarrow \infty} 0,$$

and on the other hand

$$v^2(t) = v_0^2 e^{-2\gamma t} + 2v_0 e^{-\gamma t} \int_0^t e^{-\gamma(t-s)} \eta(s) ds + \int_0^t \int_0^t e^{-\gamma(t-s)} e^{-\gamma(t-s')} \eta(s) \eta(s') ds' ds,$$

such that

$$\begin{aligned}\langle v^2(t) \rangle &= v_0^2 e^{-2\gamma t} + \int_0^t \int_0^t e^{-\gamma(t-s)} e^{-\gamma(t-s')} \Gamma \delta_0(s-s') ds' ds \\ &= v_0^2 e^{-2\gamma t} + \frac{\Gamma}{2\gamma} (1 - e^{-2\gamma t}) \xrightarrow{t \rightarrow \infty} \frac{\Gamma}{2\gamma}.\end{aligned}$$

What can be observed about these two computations is that the initial conditions are lost after some time, the mean velocity tends towards zero in the long-time asymptotics, however the mean squared velocity has a non-zero, finite limit. In the long-time limit $t \rightarrow \infty$ the Brownian particle gets in equilibrium with the surrounding medium. If this one is in thermodynamic equilibrium, characterized by a temperature T (thermal bath), the equipartition theorem of thermodynamics relates the temperature of the medium to the average kinetic energy of the particle via

$$\frac{m}{2} \langle v_\infty^2 \rangle = \frac{1}{2} k_B T \quad \Rightarrow \quad \Gamma = 2 \frac{k_B T}{m} \gamma, \quad (1.5)$$

where k_B is the so-called Boltzmann constant. In other words, in the long-time limit $\langle v^2(t) \rangle$ approaches the squared of the thermal velocity given by $v_{th} := \sqrt{\frac{k_B T}{m}}$. The identity (1.5) relates a quantity associated with the fluctuations, *i.e.* Γ , to the coefficient describing the dissipation, *i.e.* γ (fluctuation-dissipation relation). It expresses the balance between friction, which tends to drive the system towards an inactive state, and noise which tends to keep the system in mouvement.

We are now able to characterize the solution to the Langevin equation (1.1) as a Gaussian process with mean

$$\mu(t) := \langle v(t) \rangle = v_0 e^{-\gamma t}, \quad \forall t > 0, \quad (1.6)$$

and variance function

$$\sigma^2(t) := \langle [v(t) - \langle v(t) \rangle]^2 \rangle = \frac{k_B T}{m} (1 - e^{-2\gamma t}), \quad \forall t > 0. \quad (1.7)$$

In the long-time asymptotics we obtain the following equilibrium probability distribution function for the velocities of our Brownian motion

$$f_\infty(v) := \frac{1}{\sqrt{2\pi\sigma_\infty^2}} e^{-\frac{v^2}{2\sigma_\infty^2}} \quad \text{with} \quad \sigma_\infty^2 := \frac{k_B T}{m} = v_{th}^2, \quad \mu_\infty = 0, \quad (1.8)$$

which is the so-called *Maxwell-Boltzmann distribution function*.

1.2 The Fokker-Planck equation

The question is now how to obtain the probability distribution function of the velocities for each time instant t . In other words instead of focusing, as in the previous subsection, on the solution $v(t)$ to the Langevin equation (1.1), we shall be rather interested in finding an equation governing the dynamics of the velocity probability distribution

function $f(t, v)$, where $f(t, v) dv$ represents the probability to find at instant t the Brownian particle with velocity in the volume dv around v . This equation will be found by making a sort of balance between the gain and the loss terms in the velocity variable v , namely the time-fluctuations of the quantity $f(t, v)$ are given by

$$\partial_t f(t, v) = \int_{-\infty}^{\infty} [\tilde{b}(v, v') f(t, v') - \tilde{b}(v', v) f(t, v)] dv', \quad \forall (t, v) \in \mathbb{R}^+ \times \mathbb{R}, \quad (1.9)$$

where $\tilde{b}(v, v')$ is the so-called cross-section and gives the probability per unit time of a velocity transition from v' towards v . We suppose here that this cross-section is independent of time, so that memory-effects are neglected, and that only small changes in velocity can occur.

In order to remodel a little bit more the balance equation (1.9), we shall introduce the new velocity variable $y := v - v'$ which shall be considered as small when compared with v , and we shall define the new cross-section

$$b(u - w, w) := \tilde{b}(u, w), \quad \forall u, w \in \mathbb{R}.$$

Assuming the necessary regularity, we have thus

$$\begin{aligned} \partial_t f(t, v) &= \int_{-\infty}^{\infty} [b(v - v', v') f(t, v') - b(v' - v, v) f(t, v)] dv' \\ &= \int_{-\infty}^{\infty} [b(y, v - y) f(t, v - y) - b(-y, v) f(t, v)] dy \\ &= \int_{-\infty}^{\infty} [b(y, v - y) f(t, v - y) - b(y, v) f(t, v)] dy, \end{aligned}$$

where in the second term of the last line, we made the change of variable $y \rightarrow -y$. A Taylor expansion around v with $|y| \ll |v|$ yields

$$b(y, v - y) f(t, v - y) = b(y, v) f(t, v) - y \partial_v [b(y, v) f(t, v)] + \frac{y^2}{2} \partial_{vv}^2 [b(y, v) f(t, v)] + \dots$$

Recalling that b is concentrated around $y \approx 0$, we have thus altogether

$$\begin{aligned} \partial_t f(t, v) &\approx \int_{-\infty}^{\infty} \left\{ -y \partial_v [b(y, v) f(t, v)] + \frac{y^2}{2} \partial_{vv}^2 [b(y, v) f(t, v)] \right\} dy \\ &= -\partial_v \left\{ \left(\int_{-\infty}^{\infty} y b(y, v) dy \right) f(t, v) \right\} + \frac{1}{2} \partial_{vv}^2 \left\{ \left(\int_{-\infty}^{\infty} y^2 b(y, v) dy \right) f(t, v) \right\}. \end{aligned}$$

This can be rewritten as

$$\partial_t f(t, v) = -\partial_v [A(v) f(t, v)] + \frac{1}{2} \partial_{vv}^2 [B(v) f(t, v)],$$

where

$$A(v) := \int_{-\infty}^{\infty} y b(y, v) dy, \quad B(v) := \int_{-\infty}^{\infty} y^2 b(y, v) dy. \quad (1.10)$$

One can use now the expression of the solution to the Langevin equation (1.1) in order to compute $A(v)$ respectively $B(v)$ and to obtain

$$A(v) = -\gamma v, \quad B(v) = 2\gamma \frac{k_B T}{m}.$$

Indeed, replacing $y = v' - v$ in (1.10), thus $dy = dv'$, reminding that $\tilde{b}(v', v)$ is the probability per unit time of a velocity transition from v towards v' , and denoting by $v' := v(\Delta t)$ the solution of the Langevin equation (1.1) with initial condition v , then one has

$$A(v) = \lim_{\Delta t \rightarrow 0} \langle v(\Delta t) - v \rangle \frac{1}{\Delta t} = \lim_{\Delta t \rightarrow 0} v \frac{e^{-\gamma \Delta t} - 1}{\Delta t} = -\gamma v,$$

where the mean $\langle \cdot \rangle$ is taken over all realizations of the random force field $\eta(t)$. Similar computations give rise to the $B(v)$ expression. This leads finally to the Fokker-Planck equation

$$\partial_t f(t, v) = \gamma \partial_v \left[v f(t, v) + \frac{k_B T}{m} \partial_v f \right]. \quad (1.11)$$

This is a deterministic partial differential equation on the probability distribution function f , which has the form of a drift-diffusion equation in the velocity variable. Let us underline here the interpretation of $\frac{k_B T}{m}$ as a diffusion coefficient in v . The right hand side of (1.11) can be rewritten in the form $\gamma \partial_v \left[\frac{k_B T}{m} f_{eq} \partial_v \left(\frac{f}{f_{eq}} \right) \right]$, where f_{eq} is defined in (1.12). These reformulation permits to obtain in a simple manner the stationary solutions to the Fokker-Planck equation.

It is sometimes interesting to write the Fokker-Planck equation as a continuity equation

$$\partial_t f(t, v) + \partial_v \mathcal{J}(t, v) = 0,$$

with the probability current given by

$$\mathcal{J}(t, v) := -\gamma v f(t, v) - \gamma \frac{k_B T}{m} \partial_v f(t, v).$$

Integrating the continuity equation over the velocity-interval $[v_-, v_+]$ yields

$$\partial_t \int_{v_-}^{v_+} f(t, v) dv = \mathcal{J}(t, v_-) - \mathcal{J}(t, v_+),$$

which means that a change in the probability density distribution in the interval $[v_-, v_+]$ comes from changes in the current-fluxes through the boundaries.

1.3 Properties and remarks

The Fokker-Planck equation is a basic equation in many areas of physics and biology. It models a set of particles experiencing both, diffusion and drift. The interplay between these two effects is at the basis of most of its properties, which shall be briefly summarized here in a multi-dimensional framework.

Stationary solutions

If the environment of our Brownian particle is in thermal equilibrium at temperature T , then the Brownian particle is thermalized, and the stationary solutions of (1.11) are given by the Maxwell-Boltzmann distribution function

$$f_{eq}(v) := \left(\frac{m}{2\pi k_B T} \right)^{d/2} e^{-\frac{m|v|^2}{2k_B T}}, \quad \forall v \in \mathbb{R}^d. \quad (1.12)$$

We recognize the equilibrium probability function f_∞ found in (1.8) for $d = 1$.

Fundamental solutions

Another important question is to find the fundamental solutions of (1.11) if possible, the so-called Green's functions. In other words, we are searching for the solutions of the Fokker-Planck equation with initial condition given by $g(0, v; v_0) := \delta_0(v - v_0)$ for an arbitrary $v_0 \in \mathbb{R}^d$. These are given by

$$g(t, v; v_0) := \left(\frac{1}{2\pi \sigma^2(t)} \right)^{d/2} e^{-\frac{|v - \mu(t)|^2}{2\sigma^2(t)}} \quad \forall t > 0,$$

which is nothing but a Gaussian distribution with mean velocity $\mu(t)$ and spread/deviation $\sigma(t)$ given in (1.6)-(1.7). The fundamental solutions enable now to obtain the solutions of the Fokker-Planck equation (1.11) for any initial condition f_0 , namely via

$$f(t, v) = \int_{\mathbb{R}^d} g(t, v; v_0) f(v_0) dv_0.$$

Physical properties

Let us now consider the following linear Fokker-Planck equation

$$\partial_t f(t, v) = \nabla_v \cdot [v f(t, v) + \nabla_v f], \quad \forall (t, v) \in \mathbb{R}^+ \times \mathbb{R}^d,$$

and observe that it has the following characteristics:

- One conservation law

$$\partial_t \rho = 0, \quad \rho(t) := \int_{\mathbb{R}^d} f(t, v) dv.$$

- A natural Lyapunov functional, the free-energy, composed of the sum of the entropy and the kinetic energy, namely

$$\mathcal{E}(f) := \int_{\mathbb{R}^d} f \log(f) dv + \int_{\mathbb{R}^d} \frac{|v|^2}{2} f dv.$$

- The dissipation-term

$$\mathcal{D}(f)(t) := -\frac{d}{dt} \mathcal{E}(f(t)) = \int_{\mathbb{R}^d} \frac{1}{f} |\nabla_v f + v f|^2 dv \geq 0, \quad \forall t \in \mathbb{R}^+,$$

which can be rewritten as the so-called Fisher information of f with respect to the equilibrium distribution $f_{eq}(v) = \frac{1}{(2\pi)^{d/2}} e^{-\frac{|v|^2}{2}}$, namely $\mathcal{D}(f) = \mathcal{I}(f|f_{eq})$, where

$$\mathcal{I}(f|g) := \int_{\mathbb{R}^d} f \left| \nabla_v \log \left(\frac{f}{g} \right) \right|^2 dv.$$

Force field from a potential

Finally let us remark that if the particle is immersed in an exterior potential-field $\phi(x)$, yielding an additional force $F_{ext}(t, x) := -\nabla_x \phi(t, x)$, then the Fokker-Planck equations becomes space-dependent and writes

$$\partial_t f(t, x, v) + v \cdot \nabla_x f - \nabla_x \phi(t, x) \cdot \nabla_v f = \gamma \nabla_v \cdot \left[v f(t, x, v) + \frac{k_B T}{m} \nabla_v f \right]. \quad (1.13)$$

It is now possible to make use of the Sobolev inequalities, to get an estimate on the speed of return of the distribution function f towards the equilibrium f_{eq} .

Boundary conditions

When one is considering the Fokker-Planck equation in a bounded domain $\Omega \subset \mathbb{R}^d$, with boundary $\partial\Omega$ and outward unit normal vector $n(x)$, then boundary conditions have to be specified. Different boundary conditions can be imagined, as for example *reflecting boundary conditions* (impenetrable wall)

$$f(t, x, R_x v) = f(t, x, v), \quad \forall x \in \partial\Omega, \quad R_x v := v - 2(v \cdot n(x)) n(x),$$

or *absorbing boundary conditions* (absorbing wall), meaning $f(t, x, v) = 0$ for all incoming velocities v at $x \in \partial\Omega$.

In contrast with this, if $\Omega = \mathbb{R}^d$ *natural boundary conditions* are imposed, which require that the distribution function is vanishing as $|x| \rightarrow \infty$.

1.4 Variational framework for the Fokker-Planck equation

The linear Fokker-Planck equation

$$\begin{cases} \partial_t f(t, v) - \nabla_v \cdot [v f + \nabla_v f] = 0, & \forall (t, v) \in \mathbb{R}^+ \times \mathbb{R}^d, \\ f(0, \cdot) = f_{in}, \end{cases} \quad (1.14)$$

is of parabolic type and has a very nice variational framework. Introducing the weighted Hilbert-spaces

$$L_\mu^2 := \left\{ f \in L^2(\mathbb{R}^d) / \int_{\mathbb{R}^d} |f|^2 d\mu < \infty \right\}, \quad (f, g)_\mu := \int_{\mathbb{R}^d} f g d\mu, \quad (1.15)$$

$$H_\mu^1 := \{ f \in L_\mu^2 / \nabla_v f \in (L_\mu^2)^d \}, \quad (f, g)_{H_\mu^1} := (f, g)_\mu + (\nabla_v f, \nabla_v g)_\mu, \quad (1.16)$$

with measure $d\mu := \mathcal{M}^{-1} dv$ and $\mathcal{M}(v) := \frac{1}{(2\pi)^{d/2}} e^{-|v|^2/2}$, one can show that $\mathcal{Q}(f) := \nabla_v \cdot [v f + \nabla_v f]$ is a linear, bounded operator defined as

$$\mathcal{Q} : H_\mu^1 \rightarrow H_\mu^{-1}, \quad \langle \mathcal{Q}(f), g \rangle_{H_\mu^{-1}, H_\mu^1} := -(v f + \nabla_v f, v g + \nabla_v g)_\mu,$$

where H_μ^{-1} denotes the dual space of H_μ^1 . It is also important to remark that for $f \in H_\mu^1$ one has $v f \in L_\mu^2$. This can be shown in 1D via a Hermite decomposition. Indeed, defining the Hermite functions $\{\psi_k\}_{k \in \mathbb{N}}$ recursively as

$$\sqrt{k+1} \psi_{k+1}(v) = v \psi_k(v) - \sqrt{k} \psi_{k-1}(v), \quad \psi_{-1} \equiv 0, \quad \psi_0 \equiv \mathcal{M}, \quad \psi_1 \equiv v \mathcal{M},$$

these one form a complete, orthogonal basis of L^2_μ and satisfy moreover

$$\psi'_k(v) = -\sqrt{k+1}\psi_{k+1}(v), \quad \int_{-\infty}^{\infty} \psi_k(v) \psi_l(v) \mathcal{M}^{-1} dv = \delta_{kl}.$$

The solution to (1.14) can thus be uniquely decomposed as

$$f(t, v) := \sum_{k=0}^{\infty} \alpha_k(t) \psi_k(v), \quad (1.17)$$

decomposition which permits to show the desired property.

A more common mathematical framework is obtained if one rescales the distribution function f via the equilibrium distribution $\mathcal{M}(v) := \frac{1}{(2\pi)^{d/2}} e^{-|v|^2/2}$, in particular by introducing $g := f/\mathcal{M}$, which satisfies the equation

$$\begin{cases} \partial_t g - \Delta_v g + v \cdot \nabla_v g = 0, & \forall (t, v) \in \mathbb{R}^+ \times \mathbb{R}^d, \\ g(0, \cdot) = g_{in}. \end{cases} \quad (1.18)$$

Denoting the new collision operator by $\mathcal{L}(g) := \Delta_v g - v \cdot \nabla_v g$ and introducing the corresponding Hilbert-spaces with measure $d\gamma := \mathcal{M} dv$

$$\mathcal{H} := L^2_\gamma, \quad \mathcal{V} := H^1_\gamma, \quad (1.19)$$

one can show that $\mathcal{L} : \mathcal{V} \rightarrow \mathcal{V}^*$ is a linear, bounded operator defined as $\langle \mathcal{L}(f), g \rangle_{H^{-1}_\gamma, H^1_\gamma} := -(\nabla_v f, \nabla_v g)_\gamma$ for all $f, g \in H^1_\gamma$. Introducing the adjoint operator ∇_v^* of the gradient via

$$\nabla_v^* : L^2_\gamma \rightarrow H^{-1}_\gamma, \quad \nabla_v^* \xi := v \xi - \nabla_v \xi.$$

one can rewrite the collision operator in a simpler form as $\mathcal{L} = -\nabla_v^* \cdot \nabla_v$.

Proposition 1.4.1 *Reducing the collision operator \mathcal{L} to an L^2 -operator, namely to $\mathcal{L} : D(\mathcal{L}) \subset L^2_\gamma \rightarrow L^2_\gamma$, this one satisfies the following properties :*

- (i) *The linear operator $\mathcal{L} : D(\mathcal{L}) \subset \mathcal{H} \rightarrow \mathcal{H}$ is symmetric and non-positive.*
- (ii) *The kernel of \mathcal{L} is given by*

$$\text{Ker}(\mathcal{L}) := \{\rho \in \mathbb{R}\}.$$

- (iii) *The L^2_γ -orthogonal to the kernel of \mathcal{L} is*

$$(\text{Ker}(\mathcal{L}))^\perp := \left\{ f \in \mathcal{H} / \int_{\mathbb{R}^d} f(v) \mathcal{M} dv = 0 \right\},$$

and we have $L^2_\gamma = \text{Ker}(\mathcal{L}) \oplus (\text{Ker}(\mathcal{L}))^\perp$, where $f = \Pi f + (Id - \Pi) f$ with Π the orthogonal projection on the kernel of \mathcal{L} , given by

$$\Pi : L^2_\gamma \rightarrow \text{Ker}(\mathcal{L}) \quad f \mapsto \int_{\mathbb{R}^d} f(v) \mathcal{M} dv.$$

(iv) $-\mathcal{L}$ is coercive on $D(\mathcal{L}) \cap (\text{Ker}(\mathcal{L}))^\perp$, i.e.

$$-(\mathcal{L}(f), f)_\gamma = -\langle \mathcal{L}(f), f \rangle_{H_\gamma^{-1}, H_\gamma^1} \geq C \|f\|_{\mathcal{H}}^2, \quad \forall f \in D(\mathcal{L}) \cap (\text{Ker}(\mathcal{L}))^\perp.$$

(v) The range $\text{Im}(\mathcal{L})$ of \mathcal{L} is closed in L_γ^2 and coincides with $(\text{Ker}(\mathcal{L}))^\perp$. We have moreover the one-to-one mapping

$$\mathcal{L} : D(\mathcal{L}) \cap (\text{Ker}(\mathcal{L}))^\perp \rightarrow (\text{Ker}(\mathcal{L}))^\perp.$$

Introducing the bilinear form associated to $\mathcal{L} : \mathcal{V} \rightarrow \mathcal{V}^*$, namely

$$l : \mathcal{V} \times \mathcal{V} \rightarrow \mathbb{R}, \quad l(f, g) := (\nabla_v f, \nabla_v g)_\gamma,$$

one enters into the mathematical framework of the Lax-Milgram or Lions theorem, such that the well-posedness of a solution to (1.18) is a natural consequence. In more details for each $T > 0$ there exists a unique weak solution g of (1.18) satisfying

$$g \in W_2^1(0, T; \mathcal{V}, \mathcal{H}) \subset C([0, T]; \mathcal{H}).$$

For this theory one has to consider the evolution triplet $\mathcal{V} \subset \mathcal{H} = \mathcal{H}^* \subset \mathcal{V}^*$.

Chapter 2

Entropy methods

In this chapter we shall consider the following autonomous evolution equation

$$\begin{cases} \partial_t u(t) = F(u(t)), & \forall t > 0, \\ u(0) = u_0, \end{cases} \quad (2.1)$$

that describes for example the dynamics of some particle swarm. Here $F : D(F) \subset \mathcal{X} \rightarrow \mathcal{X}$ is some possible nonlinear operator on the functional Banach-space \mathcal{X} . The questions we are asking concern, apart the obvious existence and uniqueness investigations, the asymptotic long-time behaviour of the solution to this problem towards an equilibrium state $u_\infty \in \ker F$, to be identified. Entropy dissipation methods have been developed to investigate this qualitative long-time behaviour of the solutions, and are based as much as possible on physical arguments, such as dissipation processes, giving the direction of the time flow.

The notion of Lyapunov functional and entropy play a fundamental role in ODE resp. PDE theory. For example, in hyperbolic theory the entropy allows to pick up a unique (physical) weak solution within all the existent weak solutions of the considered nonlinear hyperbolic equations. In kinetic theory, the entropy is a useful tool to derive hydrodynamic equations from the underlying kinetic equations (as for ex. Boltzmann, Fokker-Planck or Landau equations) and this via the so-called H -theorem. The entropy plays also a fundamental role in the global-in-time existence proof as well as regularity proof for cross-diffusion systems, which are strongly coupled “parabolic-type” equations, with a diffusion matrix which is neither symmetric nor positive-definite, such that standard elliptic/parabolic theories does not apply any more.

Definition 2.0.1 (Lyapunov functional) *Let $\mathcal{E} : D(F) \subset \mathcal{X} \rightarrow \mathbb{R}$ be a functional decreasing along the trajectories $u(t)$ of (2.1), namely satisfying*

$$\frac{d}{dt} \mathcal{E}(u(t)) \leq 0, \quad \forall t > 0.$$

Such a functional \mathcal{E} is then called a Lyapunov functional for (2.1).

An entropy is a specific Lyapunov functional, as stated in the next definition.

Definition 2.0.2 (Entropy) We call $\mathcal{E} : D(F) \subset \mathcal{X} \rightarrow \mathbb{R}$ an entropy corresponding to (2.1), if the following properties are satisfied

- \mathcal{E} is a Lyapunov functional corresponding to (2.1);
- \mathcal{E} is convex.

The entropy is a physical quantity which has several interpretations, depending on the problem one is investigating. The entropy measures the disorder in a system (entropy of mixing), it can be identified with a measure of the ignorance about a system (information theory) or finally it can measure the irreversible changes in a system (thermodynamics).

Definition 2.0.3 (Entropy dissipation) Let \mathcal{E} be an entropy corresponding to (2.1). Then the entropy dissipation or entropy production is a functional $\mathcal{D} : D(F) \subset \mathcal{X} \rightarrow \mathbb{R}$ satisfying

$$\mathcal{D}(u(t)) = -\frac{d}{dt}\mathcal{E}(u(t)), \quad \forall t > 0,$$

along the trajectories $u(t)$ of (2.1).

In order to be able to use entropies to prove asymptotic convergence results of a solution towards an equilibrium, we need a further concept, namely the relative entropy.

Definition 2.0.4 (Relative entropy) For a given entropy \mathcal{E} and a given function u_∞ , we define the relative entropy (Bregman divergence) as follows

$$\mathcal{E}(u|u_\infty) := \mathcal{E}(u) - \mathcal{E}(u_\infty) - d\mathcal{E}(u_\infty)(u - u_\infty) \geq 0,$$

which is nothing but the first Taylor expansion of \mathcal{E} around u_∞ . The last term represents the directional derivative of \mathcal{E} ($d\mathcal{E}(u_\infty)$ being the Fréchet derivative in u_∞).

The Bregman relative entropy measures somehow the distance between two probability distributions, even if it is not a metric, as it is not symmetric, nor does it satisfy the triangle inequality. Remark that one has $\mathcal{E}(u_\infty|u_\infty) = 0$ as well as the simple expression $\mathcal{E}(u|u_\infty) = \mathcal{E}(u) - \mathcal{E}(u_\infty)$, if u_∞ is a minimizer of \mathcal{E} , meaning for u_∞ satisfying $d\mathcal{E}(u_\infty) \equiv 0$.

Very often, in kinetic theory, one defines a special kind of entropy, the *phi*-entropy, given by

$$\mathcal{E}_\phi(u) := \int_{\mathbb{R}^d} \phi(u(\cdot)) dx, \quad (2.2)$$

where the entropy generating function $\phi : \mathbb{R}^+ \rightarrow \mathbb{R}^+$ is a continuous, convex function, satisfying $\phi(1) = 0$. In this case, the relative entropy is often defined as

$$\mathcal{E}_\phi(u|u_\infty) := \int_{\mathbb{R}^d} \phi\left(\frac{u}{u_\infty}\right) u_\infty dx. \quad (2.3)$$

To give an example, the **generalized Kullback-Leibler** entropy is based on the function $\phi(x) := x \log(x) - x + 1$, yielding the Kullback-Leibler divergence

$$\mathcal{E}_\phi(u|u_\infty) := \int_{\mathbb{R}^d} \left[u(x) \log\left(\frac{u}{u_\infty}\right) - u(x) + u_\infty(x) \right] dx.$$

As a second example, we mention a Bregman-divergence which cannot be written under the form (2.2), namely taking $\mathcal{E}(u) := \|u\|_{L^2}^2$ yielding $\mathcal{E}(u|u_\infty) := \|u - u_\infty\|_{L^2}^2$, which is a standard distance.

What can be mentioned here is that there are many situations in which it is meaningful to measure the distance between two probability distributions, but the appropriate metric may depend on the field of application and has to be identified.

The problem we shall be concerned with now is not the existence/uniqueness theory of the Cauchy-problem (2.1), but rather the asymptotic behaviour of its solutions as $t \rightarrow \infty$. One may ask,

- if there is a unique equilibrium u_∞ of (2.1) (minimizer of entropy \mathcal{E} , zero of F);
- if $u(t)$ converges towards u_∞ as $t \rightarrow \infty$;
- what is the rate of convergence of $u(t)$ towards u_∞ .

Naturally, these questions require the definition of a measure, permitting to quantify the distance between $u(t)$ and u_∞ . For example this can be done in the entropy sense, by evaluating the relative entropy $\mathcal{E}(u|u_\infty)$, or in the L^1 -sense by evaluating $\|u(t) - u_\infty\|_{L^1}$.

The main strategy behind entropy methods is now the following:

- Identify the equilibrium state u_∞ and an entropy functional \mathcal{E} , associated with the problem to be treated (2.1). Define a relative entropy $\mathcal{E}(u|u_\infty)$;
- Given the entropy functional, which attains its minimum at the equilibrium state, the distance between the solution $u(t)$ and the equilibrium u_∞ can be measured by the relative entropy, namely $\mathcal{E}(u|u_\infty)$. To do this, one investigates generally the entropy dissipation or production functional $\mathcal{D}(u(t)) = -\frac{d}{dt}\mathcal{E}(u(t))$. Indeed, the main idea is that the entropy production controls the relative entropy, via some entropy-entropy production inequality of the type

$$\mathcal{D}(u(t)) = -\frac{d}{dt}\mathcal{E}(u(t)) \geq \Phi(\mathcal{E}(u|u_\infty)),$$

where Φ is a positive, continuous, strictly increasing function, satisfying $\Phi(0) = 0$. Gronwall's inequality implies then the convergence towards the equilibrium in the entropy sense, with explicit convergence rate if Φ has a simple form (exponential convergence rate for linear Φ);

- Finally, a Csiszár-Kullback inequality of the type

$$\|u(t) - u_\infty\|_{L^1} \leq \chi(\mathcal{E}(u|u_\infty)),$$

with χ a positive, continuous, strictly increasing function, satisfying $\chi(0) = 0$, permits then to show that the distance between the solution $u(t)$ and the equilibrium u_∞ is controlled by the relative entropy $\mathcal{E}(u|u_\infty)$, implying the convergence in the L^1 sense (with explicit convergence rate, if Φ and χ are simple functions).

2.1 Coercivity versus Hypo-coercivity

Let us start by introducing the concepts of coercivity and hypocoercivity of the operator $L : D(L) \subset \mathcal{H} \rightarrow \mathcal{H}$, where \mathcal{H} is a Hilbert-space endowed with the scalar product $(\cdot, \cdot)_{\mathcal{H}}$. We shall assume in this subsection that L is a linear, unbounded operator with closed range, and let us consider the following problem

$$\begin{cases} \partial_t u = -L u, & \forall t > 0, \\ u(0) = u_0. \end{cases} \quad (2.4)$$

Definition 2.1.1 (Coercivity) *The operator L is said to be λ -coercive (on $(\ker L)^\perp$) for some $\lambda > 0$, if*

$$(Lh, h)_{\mathcal{H}} \geq \lambda \|h\|_{\mathcal{H}}^2, \quad \forall h \in D(L) \cap (\ker L)^\perp. \quad (2.5)$$

If we denote by $\Pi : D(L) \subset \mathcal{H} \rightarrow \ker L$ the orthogonal projection on the kernel of L , inequality (2.5) can be rewritten as

$$(Lh, h)_{\mathcal{H}} \geq \lambda \|(Id - \Pi)h\|_{\mathcal{H}}^2, \quad \forall h \in D(L).$$

By Gronwall's lemma, λ -coercivity implies exponential convergence of the solution u of (2.1) towards the equilibrium $u_\infty = \Pi(u_0) \in \ker L$. Indeed, defining the entropy

$$\mathcal{E}(u) := \frac{1}{2} \|u\|_{\mathcal{H}}^2,$$

one gets immediately for a solution u of (2.4) with $u_0 \in D(L) \cap (\ker L)^\perp$ that

$$\frac{d}{dt} \mathcal{E}(u(t)) = -(Lu, u)_{\mathcal{H}} \leq -\lambda \|u\|_{\mathcal{H}}^2,$$

leading hence to exponential convergence towards zero, namely

$$\|u(t)\|_{\mathcal{H}} \leq e^{-\lambda t} \|u_0\|_{\mathcal{H}}, \quad \forall u_0 \in D(L) \cap (\ker L)^\perp.$$

Let us mention one simple example of a coercive operator, namely the spatially homogeneous Fokker-Planck equation

$$\partial_t f = -L_1 f, \quad L_1 f := -\partial_{vv} f + v \partial_v f,$$

where the evolution equation lives in $(t, v) \in \mathbb{R}^+ \times \mathbb{R}$, the operator L_1 is acting only on the velocity variable $v \in \mathbb{R}$ and the corresponding Hilbert-space is given by $\mathcal{H} := L^2(d\mu_\infty)$ with $d\mu_\infty := \mathcal{M} dv$ and $\mathcal{M} := \frac{1}{\sqrt{2\pi}} e^{-v^2/2}$. Considering $t \in \mathbb{R}^+$ as a parameter, one has in this case

$$(L_1 f, f)_{\mathcal{H}} = \|\partial_v f\|_{\mathcal{H}}^2 \geq C_P \|f\|_{\mathcal{H}}^2, \quad \forall f \in D(L_1) \cap (\ker L_1)^\perp,$$

where we used the weighted Poincaré's inequality as well as

$$\ker L_1 := \{c \in \mathbb{R}\}, \quad (\ker L_1)^\perp := \left\{ f \in \mathcal{H} / \int_{\mathbb{R}} f \mathcal{M} dv = 0 \right\}.$$

However in many cases, despite the fact that coercivity does not hold, the exponential decay still happens to exist. The notion of hypocoercivity is introduced for describing such exponential decay of a solution in the absence of coercivity.

Definition 2.1.2 (Hypo-coercivity) *The operator L is said to be λ -hypo-coercive (on $(\ker L)^\perp$) for some $\lambda > 0$, if there exist a constant $C > 0$ such that*

$$\|u(t)\|_{\mathcal{H}} \leq C e^{-\lambda t} \|u_0\|_{\mathcal{H}}, \quad \forall u_0 \in D(L) \cap (\ker L)^\perp.$$

The non-homogeneous Fokker-Planck equation is a typical example of a hypo-coercive operator, namely

$$\partial_t f = -L_2 f, \quad L_2 f := v \partial_x f + (-\partial_{vv} f + v \partial_v f), \quad (2.6)$$

the evolution equation living in $(t, x, v) \in \mathbb{R}^+ \times \mathbb{T} \times \mathbb{R}$, with \mathbb{T} the periodic torus and $\mathcal{H} := L^2(d\nu_\infty)$ the Hilbert-space with $d\nu_\infty := \mathcal{M} dx dv$ and $\mathcal{M} := \frac{1}{\sqrt{2\pi}} e^{-v^2/2}$. Let us observe also that we have

$$\ker L_2 := \{c \in \mathbb{R}\}, \quad (\ker L_2)^\perp := \left\{ f \in \mathcal{H} / \int_{\mathbb{R}} \int_{\mathbb{T}} f \mathcal{M} dx dv = 0 \right\}.$$

In this case we have to modify the entropy, in order to get an estimate of the rate of convergence. Indeed, with the standard entropy $\mathcal{E}(f) := \frac{1}{2} \|f\|_{\mathcal{H}}^2$ one can only get

$$\frac{d}{dt} \left(\frac{1}{2} \|f\|_{\mathcal{H}}^2 \right) = -\|\partial_v f\|_{\mathcal{H}}^2 \leq -C_P \|f - \langle f \rangle\|_{\mathcal{H}}^2, \quad \langle f \rangle(t, x) := \int_{\mathbb{R}} f(t, x, v) \mathcal{M} dv,$$

and we do not recover the whole entropy on the right, which would permit to get the desired exponential decay. A better choice would be to consider the modified entropy

$$\mathcal{G}(f) := \alpha \|f\|_{\mathcal{H}}^2 + \beta \|\partial_v f\|_{\mathcal{H}}^2 + \|\partial_x f\|_{\mathcal{H}}^2 + \delta (\partial_v f, \partial_x f)_{\mathcal{H}},$$

with α, β, δ positive constants to be chosen such that \mathcal{G} is decreasing along the trajectories f of (2.6). The introduction of the additional term $(\partial_v f, \partial_x f)_{\mathcal{H}}$ proves to be helpful to prove the exponential decay, as it introduces some mixing between the two space and velocity variables x and v . It is important to understand here that it is the combination of both, on one hand the transport term $v \partial_x f$, which mixes the space and the velocity variable, and on the other hand the Fokker-Planck term $-\partial_{vv} f + v \partial_v f$ which regularizes and dissipates in the velocity variable, which leads finally to the decay and regularity in both variables, and these two effects are now somehow taken into account with the additional ‘‘mixing term’’.

Let us first prove that \mathcal{G} is equivalent to the $H^1(d\nu_\infty)$ norm, defined by $\|f\|_{\mathcal{H}^1}^2 := \|f\|_{\mathcal{H}}^2 + \|\partial_x f\|_{\mathcal{H}}^2 + \|\partial_v f\|_{\mathcal{H}}^2$, for some well-chosen constants $\alpha, \beta, \delta > 0$.

Lemma 2.1.3 *If $\delta^2 < \beta$ then there exist two constants $c_1, c_2 > 0$ such that*

$$c_1 \|f\|_{\mathcal{H}^1}^2 \leq \mathcal{G}(f) \leq c_2 \|f\|_{\mathcal{H}^1}^2.$$

Proof: The Cauchy-Schwarz inequality permits to show that

$$|\delta (\partial_v f, \partial_x f)_{\mathcal{H}}| \leq \frac{\delta^2}{2} \|\partial_v f\|_{\mathcal{H}}^2 + \frac{1}{2} \|\partial_x f\|_{\mathcal{H}}^2,$$

thus

$$\alpha \|f\|_{\mathcal{H}}^2 + \left(\beta - \frac{\delta^2}{2}\right) \|\partial_v f\|_{\mathcal{H}}^2 + \frac{1}{2} \|\partial_x f\|_{\mathcal{H}}^2 \leq \mathcal{G}(f) \leq \alpha \|f\|_{\mathcal{H}}^2 + \left(\beta + \frac{\delta^2}{2}\right) \|\partial_v f\|_{\mathcal{H}}^2 + \frac{3}{2} \|\partial_x f\|_{\mathcal{H}}^2.$$

■

Let us now prove the exponential decay in the modified entropy sense.

Theorem 2.1.4 [31] *There exist positive constants α, β, δ as well as $\kappa > 0$ such that the entropy \mathcal{G} decreases along the trajectories of the Fokker-Planck equation, for all $f_0 \in \mathcal{H}^1$ satisfying $\int_{\mathbb{T}} \int_{\mathbb{R}} f_0 \mathcal{M} dv dx = 0$, namely one has*

$$\mathcal{G}(f(t)) \leq e^{-\kappa t} \mathcal{G}(f_0), \quad \forall t > 0.$$

As a consequence, there exists a constant $\nu > 0$ such that the solution to (2.6) satisfies

$$\|f(t)\|_{\mathcal{H}^1} \leq \nu e^{-\frac{\kappa}{2} t}, \quad \forall t > 0.$$

Proof: The proof is based on the evaluation of $\frac{d}{dt} \mathcal{G}(f(t))$, in particular one can show that

$$\frac{d}{dt} \mathcal{G}(f(t)) \leq -\frac{\delta}{2} (\|\partial_v f\|_{\mathcal{H}}^2 + \|\partial_x f\|_{\mathcal{H}}^2) \leq -\kappa \mathcal{G}(f(t)),$$

assuming that $1 < \delta < \beta < \alpha$, $\delta^2 < \beta$ and $\frac{1}{2}(2\beta + \delta)^2 < \alpha$ as well as using the inhomogeneous Poincaré's inequality (4.1). Gronwall's lemma and the equivalence of the norms permit to conclude the proof. ■

Remark 2.1.5 *Let us underline here the L^2 -framework of the first, coercive example, and the H^1 -framework of the second, hypocoercive example. It is also possible (but more complicated) to remain in the L^2 -framework even for the hypocoercive L_2 -operator, by considering the different modified entropy $\mathcal{G}(f(t)) := \frac{1}{2} \|f\|_{\mathcal{H}}^2 + (Af, f)_{\mathcal{H}}$, with an operator $A : \mathcal{H} \rightarrow \mathcal{H}$ which has been defined in [3].*

Let us conclude this section by giving some references in the domain of entropy methods. One can cite for instance the very complete work [6], which relates entropy methods with the Bakry-Émery calculus, and discusses the sharpness of convex Sobolev inequalities associated with general Fokker-Planck type equations. This latter discussion is very relevant when one is interested in getting optimal rates of convergence.

About the entropies constructed in the context of hypocoercive models, one can cite the review [40], which addresses many aspects of hypocoercivity in details, and in a very general setting. Therein are discussed the construction of entropies equivalent to a H^1 -norm, as we discussed in this document. However in [40], the author also discusses methods working in an L^2 -setting, as well as in a weaker, free-energy setting. The theory for hypocoercivity in a H^{-1} -setting is a very recent development, started in [5].

For specific references in hypocoercive entropy construction in the L^2 -setting, a very important reference is [27], giving a general method for the construction of entropies in abstract settings. This analysis is however limited to the case of equations with only one conservation law (such as the linear Fokker-Planck equation discussed above). This limitation is however partially removed in the more recent works [2, 13].

2.2 Two simple, linear algebraic examples

Let us illustrate with two simple toy models the essential features of the coercive resp. hypocoercive entropy-method. We consider the system

$$U'(t) = -AU(t), \quad U(t) := (x(t), y(t))^t, \quad t \in \mathbb{R},$$

with the initial condition $U(0) = U_0$ and the coercive resp. hypocoercive matrices (on $(\ker A)^\perp$)

$$A_c = \begin{pmatrix} 1 & -1 \\ -1 & 1 \end{pmatrix}, \quad A_{hc} = Q - T = \begin{pmatrix} 0 & 0 \\ 0 & 1 \end{pmatrix} - \begin{pmatrix} 0 & k \\ -k & 0 \end{pmatrix},$$

where Q corresponds to a type of collision operator (degenerate diffusion operator), whereas T corresponds to a skew-adjoint transport operator.

Coercive case: The matrix A_c admits two eigenvalues $\lambda_1 = 0$ and $\lambda_2 = 2$ with corresponding eigenvectors $v_1 = (1, 1)^t$ and $v_2 = (1, -1)^t$. Furthermore one has

$$\ker A_c := \text{span}(v_1), \quad (\ker A_c)^\perp = \text{span}(v_2).$$

Taking as entropy the functional $\mathcal{E}(U) := \frac{1}{2} \|U\|^2$ we get immediately

$$\frac{d}{dt} \mathcal{E}(U(t)) = -2 \|U(t)\|^2 = -4 \mathcal{E}(U(t)), \quad \forall U_0 \in (\ker A_c)^\perp,$$

thus, we are in a typical coercive case, which yields immediately

$$\mathcal{E}(U(t)) = e^{-4t} \mathcal{E}(U_0), \quad \|U(t)\| = e^{-2t} \|U_0\|, \quad \forall U_0 \in (\ker A_c)^\perp,$$

which is finally in accordance with the exact solution, which is

$$U(t) = \alpha v_1 + \beta e^{-2t} v_2, \quad \text{where } \alpha v_1 + \beta v_2 = U_0.$$

Hypocoercive case: Let us assume that $|k| > 1$. Then, the matrix A_{hc} admits the two complex conjugate eigenvalues and corresponding eigenvectors given by

$$\lambda_{1/2} = \frac{1}{2} \pm \mathbf{i} \frac{\sqrt{4k^2 - 1}}{2}, \quad v_{1/2} = (k, -\lambda_{1/2})^t.$$

Furthermore one has $\ker A_{hc} = \{0\}$ and $(\ker A_{hc})^\perp = \mathbb{R}^2$. Choosing as entropy functional $\mathcal{E}(U) := \frac{1}{2} \|U\|^2$ would be not enough, as

$$\frac{d}{dt} \mathcal{E}(U(t)) = -y^2(t), \quad U(t) = (x(t), y(t))^t,$$

and we have no coercivity on $\mathbb{R}^2 = (\ker A_{hc})^\perp$. However, if one takes a look at the exact solution in this case, which reads

$$U(t) = \alpha e^{-at} [\sin(bt + \beta) u + \cos(bt + \beta) v], \quad U_0 = \alpha [\sin(\beta) u + \cos(\beta) v],$$

with $\lambda_{1,2} = a \pm \mathbf{i}b$ and $v_{1,2} = u \pm \mathbf{i}v$, we observe an exponential decay. Thus, let us modify the entropy, adding a corrector term as

$$\mathcal{G}(U) := \frac{1}{2} \|U\|^2 + \varepsilon \frac{k}{1+k^2} x(t)y(t),$$

with the parameter $\varepsilon \in (0, 1)$ to be adequately chosen, and try to show the exponential decay in this new modified entropy sense.

Firstly, one can show that $\mathcal{G}(U)$ is equivalent to the standard $\|\cdot\|$ norm, in particular one has

$$\frac{1-\varepsilon}{2} \|U\|^2 \leq \mathcal{G}(U) \leq \frac{1+\varepsilon}{2} \|U\|^2.$$

Indeed, for $k \geq 1$ one can show that

$$\frac{1}{2} \left(1 - \varepsilon \frac{k}{1+k^2}\right) \|U(t)\|^2 \leq \frac{1}{2} \left(1 - \varepsilon \frac{k}{1+k^2}\right) \|U(t)\|^2 + \frac{k}{1+k^2} \frac{\varepsilon}{2} |x(t)+y(t)|^2 = \mathcal{G}(U),$$

and

$$\mathcal{G}(U) = \frac{1}{2} \left(1 + \varepsilon \frac{k}{1+k^2}\right) \|U(t)\|^2 - \frac{k}{1+k^2} \frac{\varepsilon}{2} |x(t)-y(t)|^2 \leq \frac{1}{2} \left(1 + \varepsilon \frac{k}{1+k^2}\right) \|U(t)\|^2,$$

where one observes that $\sup_{k \geq 1} \frac{k}{1+k^2} = \frac{1}{2} \leq 1$. Similar arguments for $k \leq -1$ yield the desired result.

Secondly, one can show the existence of some $\kappa > 0$, such that one has

$$\frac{d}{dt} \mathcal{G}(U(t)) \leq -\kappa \mathcal{G}(U(t)) \quad \Rightarrow \quad \mathcal{G}(U(t)) \leq e^{-\kappa t} \mathcal{G}(U_0),$$

using Gronwall's lemma. To see this, remark that $\frac{1}{2} \leq \frac{k^2}{1+k^2} \leq 1$ and

$$\begin{aligned} \frac{d}{dt} \mathcal{G}(U) &= -\varepsilon \frac{k^2}{1+k^2} x^2 - \left(1 - \varepsilon \frac{k^2}{1+k^2}\right) y^2 - \varepsilon \frac{k}{1+k^2} xy \\ &\leq -\frac{\varepsilon}{2} x^2 - (1-\varepsilon) y^2 + \frac{\varepsilon}{2} |x| |y| \leq -\frac{\varepsilon}{2} (1-\lambda^2) x^2 - \left(1 - \varepsilon - \frac{\varepsilon}{8\lambda^2}\right) y^2, \end{aligned}$$

for any $\lambda \in (0, 1)$. For sufficiently small $\varepsilon \in (0, 1)$ one finds the desired constant $\kappa > 0$.

Altogether, one has the exponential decay of $\|U(t)\|$ by equivalence of the norms.

2.3 The heat equation (coercive case)

Let us give here an example of the use of the entropy method for investigating the long-time asymptotics of the heat equation

$$\begin{cases} \partial_t u(t, x) = \Delta u, & \forall (t, x) \in \mathbb{R}^+ \times \mathbb{T}^d, \\ u(0, \cdot) = u_0, \end{cases} \quad (2.7)$$

where \mathbb{T}^d is the d -dimensional torus with $d \in \{1, 2, 3\}$. Let us suppose that $u_0 \in L^2(\mathbb{T}^d)$ is non-negative and define $\bar{u} := \int_{\mathbb{T}^d} u_0(x) dx$. Then problem (2.7) admits a unique smooth, global, non-negative solution, conserving the mass, namely satisfying $\int_{\mathbb{T}^d} u(t, x) dx = \int_{\mathbb{T}^d} u_0(x) dx = \bar{u}$ for all $t > 0$. Furthermore we observe that $u_\infty := \bar{u}/\text{meas}(\mathbb{T}^d)$ is the unique stationary solution of (2.7). The questions one asks now are:

- Does $u \rightarrow_{t \rightarrow \infty} u_\infty$? In which norm?
- What is the convergence rate towards the equilibrium?

To answer these questions, we introduce now the two functionals

$$H_1[u] := \int_{\mathbb{T}^d} u \log \left(\frac{u}{u_\infty} \right) dx, \quad H_2[u] := \frac{1}{2} \int_{\mathbb{T}^d} (u - u_\infty)^2 dx. \quad (2.8)$$

Firstly one observes that both are non-negative functionals. Indeed, the fact that for all $z \geq 0$ one has $z \log(z) + 1 - z \geq 0$ implies that

$$0 \leq \int_{\mathbb{T}^d} \left(u \log \left(\frac{u}{u_\infty} \right) + u_\infty - u \right) dx = \int_{\mathbb{T}^d} u \log \left(\frac{u}{u_\infty} \right) dx + \int_{\mathbb{T}^d} u_\infty dx - \int_{\mathbb{T}^d} u dx = H_1[u].$$

Secondly both functionals are Lyapunov functionals along the solutions of the heat equation (2.7). Indeed, let us start with $H_2[u]$. One has

$$\frac{dH_2}{dt}[u(t)] = \int_{\mathbb{T}^d} (u - u_\infty) \partial_t u dx = \int_{\mathbb{T}^d} (u - u_\infty) \Delta u dx = - \int_{\mathbb{T}^d} |\nabla u|^2 dx \leq 0,$$

showing that $H_2[u]$ is indeed decreasing along the trajectories of (2.7). The next step is to study if and how the solution to (2.7) converges in the long-time towards an equilibrium solution, which is u_∞ . For this asymptotic study we shall make use of the Poincaré inequality

$$\|u - \frac{1}{|\Omega|} \int_{\Omega} u dx\|_{L^2(\Omega)}^2 \leq C_P \|\nabla u\|_{L^2(\Omega)}^2 \quad \forall u \in H^1(\Omega),$$

with $\Omega \subset \mathbb{R}^d$ a bounded smooth domain. This Poincaré inequality shall indeed permit to relate the entropy $H_2[u]$ with the entropy-dissipation $\mathcal{D}_2[u(t)] := -\frac{dH_2}{dt}[u(t)]$, as follows

$$\frac{dH_2}{dt}[u(t)] = -\|\nabla u\|_{L^2(\mathbb{T}^d)}^2 \leq -C_P^{-1} \|u - u_\infty\|_{L^2(\mathbb{T}^d)}^2 = -2C_P^{-1} H_2[u(t)].$$

Gronwall's inequality yields then

$$\frac{1}{2} \|u - u_\infty\|_{L^2(\mathbb{T}^d)}^2 = H_2[u(t)] \leq e^{-2t/C_P} H_2[u_0] \quad \forall t > 0,$$

which means that we have indeed the exponential decay of $u(t)$ towards the equilibrium $u_\infty := \bar{u}/\text{meas}(\mathbb{T}^d)$ in the L^2 -sense, with rate $1/C_P$.

Let us remark here that in this L^2 -periodic framework we know the exact solution of (2.7), which reads

$$u(t, \cdot) = \sum_{k=1}^{\infty} e^{-\lambda_k t} (u_0, v_k)_{L^2} v_k, \quad \forall t \geq 0,$$

where $\{\lambda_k, v_k\}_{k \in \mathbb{N}}$ are the eigenvalues resp. associated eigenvectors of the operator $-\Delta$, associated with periodic boundary conditions. The eigenvalues form a positive, increasing sequence of real numbers, satisfying $\lambda_k \rightarrow_{k \rightarrow \infty} \infty$ whereas $\{v_k\}_{k \in \mathbb{N}}$ form an orthonormal basis of $L^2(\mathbb{T}^d)$.

Remarking that $\lambda_1 \equiv 0$, $v_1 \equiv cst.$ and $\bar{v}_k = \int_{\Omega} v_k dx = 0$ for $k \neq 1$, we have $u_{\infty} = (u_0, v_1)_{L^2} v_1$, such that

$$\|u - u_{\infty}\|_{L^2(\Omega)}^2 = \sum_{k=2}^{\infty} e^{-2\lambda_k t} (u_0, v_k)_{L^2}^2 \leq e^{-2\lambda_2 t} \|u_0\|_{L^2(\Omega)}^2,$$

which gives also the desired exponential decay, with rate λ_2 . To compare the two convergence rates, observe that in the 1D case $C_P = \mu_2^{-1}$, with $\mu_2 = \pi^2/|\mathbb{T}|^2$ the smallest possible positive eigenvalue of the Laplacian with Neumann boundary conditions, and $\lambda_2 = \pi^2/|\mathbb{T}|^2$.

Let us now change the functional and try to show the same, however considering $H_1[u]$. Firstly we have

$$\frac{dH_1}{dt}[u(t)] = \int_{\mathbb{T}^d} \left(\log \left(\frac{u}{u_{\infty}} \right) + 1 \right) \partial_t u dx = - \int_{\mathbb{T}^d} \nabla \left[\log \left(\frac{u}{u_{\infty}} \right) \right] \nabla u dx = -4 \int_{\mathbb{T}^d} |\nabla \sqrt{u}|^2 dx,$$

showing that $H_1[u]$ is decreasing along the trajectories of (2.7). To relate now the entropy with the entropy-dissipation, we shall need no more the Poincaré inequality, but this time the logarithmic Sobolev inequality

$$\int_{\Omega} u \log \left(\frac{u}{u_{\infty}} \right) dx \leq C_L \int_{\Omega} |\nabla \sqrt{u}|^2 dx \quad \forall \sqrt{u} \in H^1(\Omega), \quad u \geq 0,$$

with $\Omega \subset \mathbb{R}^d$ a bounded domain. This inequality permits indeed to get the following estimates

$$\frac{dH_1}{dt}[u(t)] = -4 \|\nabla \sqrt{u}\|_{L^2(\mathbb{T}^d)}^2 \leq -4C_L^{-1} H_1[u(t)] \quad \Rightarrow \quad H_1[u(t)] \leq e^{-4t/C_L} H_1[u_0] \quad \forall t > 0,$$

which shows that in the limit of large times $H_1[u(t)] \rightarrow_{t \rightarrow \infty} H_1[u_{\infty}] = 0$. To show the exponential decay of $u(t)$ in the Lebesgue measure sense, we shall need now the Csiszár-Kullback inequality

$$\|u - u_{\infty}\|_{L^1(\Omega)}^2 \leq C (H_1[u(t)] - H_1[u_{\infty}]),$$

which yields an exponential decay in the L^1 -sense.

Remark 2.3.1 *Let us underline at this point the two strategies used for the heat equation and leading both to an exponential decay of the solution towards the equilibrium solution, however in different norms. The "energy-strategy" based on the $H_2[u]$ Lyapunov functional, leads via Poincaré's and Gronwall's inequalities to an L^2 -exponential decay, and the "entropy-method" based on the $H_1[u]$ Lyapunov functional, which needs the Csiszár-Kullback inequality to get an L^1 -exponential decay.*

2.4 Fokker-Planck equation

In this section we shall come back towards the examples proposed in section 2.1 and shall treat them via an "entropy-strategy" rather than the "energy-strategies" proposed there.

2.4.1 The homogeneous Fokker-Planck equation (coercive case)

As a second example, let us consider the following linear Fokker-Planck equation

$$\begin{cases} \partial_t f &= \nabla_v \cdot (v f + \nabla_v f), & \forall (t, v) \in \mathbb{R}^+ \times \mathbb{R}^d, \\ f(0, \cdot) &= f_0. \end{cases} \quad (2.9)$$

The unique stationary state of this equation is given by the Maxwellian

$$f_\infty(v) := c_\star \mathcal{M}(v) = \frac{c_\star}{(2\pi)^{d/2}} e^{-|v|^2/2} \quad \forall v \in \mathbb{R}^d, \quad c_\star := \int_{\mathbb{R}^d} f_0 dv.$$

Defining the entropy

$$H_1[f] := \int_{\mathbb{R}^d} f \log \left(\frac{f}{\mathcal{M}} \right) dv,$$

we have the following theorem

Theorem 2.4.1 [32] **(Exponential decay of the Fokker-Planck equation)**

Let $f_0 \in L^1(\mathbb{R}^d)$ be a non-negative function satisfying the condition $\int_{\mathbb{R}^d} f_0 dv = 1$, and let us denote by f the corresponding unique solution to (2.9). Then the functional $H_1[f]$ is an entropy for the Fokker-Planck equation and we have

$$0 \leq H_1[f(t)] \leq e^{-2t} H_1[f_0], \quad \forall t > 0.$$

Furthermore $f(t, \cdot)$ converges in the L^1 -sense exponentially fast in the long-time limit towards the equilibrium \mathcal{M} , as

$$\|f(t, \cdot) - \mathcal{M}\|_{L^1(\mathbb{R}^d)} \leq e^{-t} \sqrt{8 H_1[f_0]}, \quad \forall t > 0.$$

Proof: Let us firstly show that $H_1[f]$ is a Lyapunov functional along the trajectories of (2.9). For this, we observe that

$$\begin{aligned} \frac{dH_1}{dt}[f(t, \cdot)] &= \int_{\mathbb{R}^d} \partial_t f \left[\log \left(\frac{f}{\mathcal{M}} \right) + 1 \right] dv = \int_{\mathbb{R}^d} \partial_t f \log \left(\frac{f}{\mathcal{M}} \right) dv \\ &= \int_{\mathbb{R}^d} \nabla_v \cdot \left[\mathcal{M} \nabla_v \left(\frac{f}{\mathcal{M}} \right) \right] \log \left(\frac{f}{\mathcal{M}} \right) dv \\ &= - \int_{\mathbb{R}^d} \frac{\mathcal{M}^2}{f} \left| \nabla_v \left(\frac{f}{\mathcal{M}} \right) \right|^2 dv = - \int_{\mathbb{R}^d} f \left| \nabla_v \log \left(\frac{f}{\mathcal{M}} \right) \right|^2 dv \leq 0. \end{aligned}$$

We used for this the fact that the collision operator can be rewritten as $\nabla_v \cdot (v f + \nabla_v f) = \nabla_v \cdot [\mathcal{M} \nabla_v (\frac{f}{\mathcal{M}})]$. Finally, the following logarithmic Sobolev inequality (see Section 4.3)

$$\int_{\mathbb{R}^d} f \left| \nabla_v \log \left(\frac{f}{\mathcal{M}} \right) \right|^2 dv \geq 2 \int_{\mathbb{R}^d} f \log \left(\frac{f}{\mathcal{M}} \right) dv,$$

permits to relate the entropy $H_1[f(t)]$ with the entropy dissipation $\mathcal{D}_1[f(t, \cdot)] := -\frac{dH_1}{dt}[f(t, \cdot)]$. Indeed, we obtain thus

$$\frac{dH_1}{dt}[f(t, \cdot)] \leq -2H_1[f(t, \cdot)].$$

Gronwall's inequality yields then the exponential decay of the solution to (2.9) in the entropy sense. Finally the Csiszár-Kullback inequality permits to show the corresponding exponential decay in the L^1 -sense, and we conclude the proof. \blacksquare

2.4.2 The inhomogeneous Fokker-Planck equation (hypocoercive case)

To compare, let us consider now the inhomogeneous Fokker-Planck equation

$$\begin{cases} \partial_t f + v \cdot \nabla_x f - \nabla_x \vartheta(x) \cdot \nabla_v f &= \nabla_v \cdot (v f + \nabla_v f), & \forall (t, x, v) \in \mathbb{R}^+ \times \mathbb{R}^d \times \mathbb{R}^d, \\ f(0, x, v) &= f_0(x, v), \end{cases} \quad (2.10)$$

where ϑ is supposed to be a known smooth potential, which is strictly convexe at infinity, for ex. let us assume here that ϑ has the form

$$\vartheta(x) := \omega_0^2 \frac{|x|^2}{2} + \Phi(x) + \vartheta_0, \quad \text{with } \vartheta_0 \in \mathbb{R}, \quad \Phi(x) \xrightarrow{x \rightarrow \infty} 0 \text{ smooth.}$$

The unique steady-state of this equation is given now by

$$f_\infty(x, v) := e^{-\vartheta(x)} \mathcal{M}(v) = \frac{e^{-\vartheta(x)}}{(2\pi)^{d/2}} e^{-|v|^2/2}, \quad \forall (x, v) \in \mathbb{R}^d \times \mathbb{R}^d.$$

The asymptotic long-time behaviour of the unique solution to (2.10) towards this equilibrium is given by the next theorem. The fact that the Fokker-Planck collision operator (right hand side of (2.10)) acts only on the velocity variable leads to a degeneracy in the x -variable, making it very hard to estimate the speed of spatial homogenization. There will be a huge family of local Maxwellians, making the entropy vanish, such that the usual H -theorem will no more give the necessary information about the long-time asymptotics, in particular it gives no indication about how to pass from a local towards the global equilibrium. Both effects, collisions and transport have to be considered in a combined manner.

Theorem 2.4.2 [25] *Let the initial distribution function f_0 be such that there exist some constants $\gamma, \Gamma > 0$ so that we have*

$$\gamma f_\infty(x, v) \leq f_0(x, v) \leq \Gamma f_\infty(x, v), \quad \forall (x, v) \in \mathbb{R}^d \times \mathbb{R}^d,$$

and let f be the unique solution to (2.10). Then for every $\varepsilon > 0$ there exists a constant $C_\varepsilon(f_0)$ depending on ε, f_0 and ϑ such that

$$\|f(t) - f_\infty\|_{L^1(\mathbb{R}_x^d \times \mathbb{R}_v^d)} \leq C_\varepsilon(f_0) t^{-1/\varepsilon}, \quad \forall t \geq 0.$$

Proof: The starting point of our proof will be the H -theorem. For this, let us define the relative entropy

$$H[f|f_\infty] := \int_{\mathbb{R}_x^d \times \mathbb{R}_v^d} f \log \left(\frac{f}{f_\infty} \right) dx dv,$$

and show that it is indeed a Lyapunov functional along the trajectories of (2.10). Indeed, we remark that

$$\frac{dH}{dt}[f|f_\infty] = - \int_{\mathbb{R}_x^d \times \mathbb{R}_v^d} f \left| \nabla_v \log \left(\frac{f}{f_\infty} \right) \right|^2 dx dv = - \int_{\mathbb{R}_x^d \times \mathbb{R}_v^d} f \left| \nabla_v \log \left(\frac{f}{\mathcal{M}} \right) \right|^2 dx dv \leq 0.$$

The entropy-dissipation vanishes only for functions of the form $f = \rho(t, x)\mathcal{M}$, with $\rho(t, x)$ arbitrary, satisfying only

$$\rho(t, x) = \int_{\mathbb{R}_v^d} f(t, x, v) dv, \quad \forall x \in \mathbb{R}^d.$$

In other words, $\rho(t, x)$ is the macroscopic density associated to the distribution function f . The functions $\rho(t, x)\mathcal{M}$ are the so-called local equilibria of (2.10), which make the right-hand side (the collision operator) of the Fokker-Planck equation vanish.

The logarithmic/convex Sobolev inequality (4.2) permits now to relate the entropy dissipation $\mathcal{D}(t) := -\frac{dH}{dt}$ to the entropy H . Indeed, one has for the so-called Fisher information $I_v[f|\rho\mathcal{M}]$

$$\begin{aligned} I_v[f|\rho\mathcal{M}] &:= \int_{\mathbb{R}_x^d \times \mathbb{R}_v^d} f \left| \nabla_v \log \left(\frac{f}{\rho\mathcal{M}} \right) \right|^2 dx dv \\ &= \int_{\mathbb{R}_x^d} \rho(x) \left(\int_{\mathbb{R}_v^d} \frac{f}{\rho(x)} \left| \nabla_v \log \left(\frac{f}{\rho\mathcal{M}} \right) \right|^2 dv \right) dx \\ &\geq 2 \int_{\mathbb{R}_x^d} \rho(x) \left(\int_{\mathbb{R}_v^d} \frac{f}{\rho(x)} \log \left(\frac{f}{\rho\mathcal{M}} \right) dv \right) dx = 2H[f|\rho\mathcal{M}]. \end{aligned}$$

Thus, we have

$$-\frac{dH}{dt}[f|f_\infty] \geq 2H[f|\rho\mathcal{M}], \quad \forall t \geq 0.$$

The crucial point is that we have on the right hand side $H[f|\rho\mathcal{M}]$ and not $H[f|f_\infty]$ as in the coercive case, which would conclude the proof via Gronwall's inequality. In the present case, the last inequality permits only to show that in the long-time limit $t \rightarrow \infty$ the distribution function f will look more and more like a local Maxwellian $\rho_\infty\mathcal{M}$, however nothing is known on the shape of $\rho_\infty(x)$. The difference between the two relative entropies, corresponding to the global as well as the local equilibria is given by

$$H[f|f_\infty] - H[f|\rho\mathcal{M}] = H_x[\rho|e^{-\vartheta}], \quad H_x[\rho|e^{-\vartheta}] := \int_{\mathbb{R}_x^d} \rho \log \left(\frac{\rho}{e^{-\vartheta}} \right) dx,$$

which is nothing but the relative entropy of ρ with respect to $e^{-\vartheta}$.

To prove the convergence of f towards the global equilibrium f_∞ one has to use more information coming from f , namely that f is the unique solution to the Fokker-Planck equation (2.10), and that f does not get stuck too close to a local Maxwellian. Let us remark here that among all local equilibria $\rho\mathcal{M}$, only one satisfies equation (2.10). Indeed, a solution $\rho(t, x)\mathcal{M}(v)$ must verify

$$\partial_t \rho + v \cdot [\nabla_x \rho + \rho \nabla_x \vartheta] = 0,$$

so that separately $\partial_t \rho = 0$ and $\nabla_x \rho = -\rho \nabla_x \vartheta$, which finally yields $f = f_\infty$ in the long-time limit. The trend towards the global equilibrium is a struggle between the collision operator (dissipation) and the anti-symmetric transport operator. The collisions push the system towards a local equilibrium $\rho(t, x)\mathcal{M}(v)$, the transport part will drive it out of this local equilibrium, if it is not the “right” one, namely the global Maxwellian.

To finish the proof, let us define now the quantities

$$x(t) := H[f(t)|f_\infty], \quad y(t) := H[f(t)|\rho(t)\mathcal{M}], \quad \forall t \geq 0.$$

One can show (rather lengthy and tricky computations) that for some $\varepsilon \in (0, 1)$ these positive quantities are solutions of the following system of differential equations, with some constants $A_1, A_2, A_3 > 0$ dependent only on ε, f_0 and ϑ

$$\begin{cases} -x'(t) & \geq A_1 y(t) \\ y''(t) + A_2 y^{1-\varepsilon}(t) & \geq A_3 x(t) \end{cases}, \quad \forall t \geq 0.$$

Then, it can be shown that there exists a constant $C_\varepsilon(f_0)$ such that

$$x(t) = H[f(t)|f_\infty] \leq C_\varepsilon(f_0) t^{-1/\varepsilon}, \quad \forall t \geq 0.$$

The Csiszár-Kullback inequality permits finally to conclude the proof. ■

Remark 2.4.3 *This entropy method seems to fail to give the optimal rate of convergence, in particular to give exponential rate of convergence towards the equilibrium. Its advantage however, as compared to the energy-methods, is that it is rather robust and the best approach to treat non-linear problems.*

2.5 The three-zone model (hypocoercive case)

In this last part of the chapter, we shall prove Theorem 0.4.5 which gives the asymptotic flocking result for the three-zone model

$$\begin{cases} x'_i(t) = v_i(t), \\ v'_i(t) = \frac{1}{N} \sum_{j=1}^N \psi(|x_i - x_j|) (v_j - v_i) - \frac{1}{N} \sum_{j=1, j \neq i}^N \nabla_{x_i} [\varphi(|x_i - x_j|)], \end{cases} \quad \forall i = 1, \dots, N, \quad (2.11)$$

and we shall discuss in a second time the property of the exponential decay rate of the solution towards the equilibrium configuration.

Proof: To prove Theorem 0.4.5, we recall firstly that we consider a bounded alignment potential ψ_b of type (7), an unbounded attraction/repulsion potential φ satisfying (9) and that we translated the system, such that

$$x_c(t) \equiv 0, \quad v_c(t) \equiv 0, \quad \forall t \in \mathbb{R}^+.$$

The existence and uniqueness of a maximal solution of (2.11) is then a simple consequence of the local Cauchy-Lipschitz theorem. To obtain a global solution, we need to show that the solution is not “exploding” in finite time, which shall be done next.

The main quantity permitting to investigate the long-time behaviour of the particle cloud is the total energy of the system, given by

$$\mathcal{E}(t) := \frac{1}{2} \sum_{i=1}^N |v_i(t)|^2 + \frac{1}{2N} \sum_{i=1}^N \sum_{j=1, j \neq i}^N \varphi(r_{ij}) = \mathcal{K}(t) + \mathcal{P}(t), \quad (2.12)$$

where $\mathcal{K}(t)$ represents the kinetic energy and $\mathcal{P}(t)$ the potential energy of the whole particle system. Simple computations permit to show that $\mathcal{E}(t)$ is a Lyapunov functional along the trajectories of (2.11). Indeed, one gets

$$\frac{d\mathcal{E}}{dt}(t) = -\frac{1}{2N} \sum_{i=1}^N \sum_{j=1, j \neq i}^N \psi_b(r_{ij}) |v_j(t) - v_i(t)|^2 \leq 0, \quad (2.13)$$

thus \mathcal{E} is decaying along the solutions of (2.11). The attraction-repulsion term describes a Hamiltonian dynamics and therefore preserves the total energy. The alignment term causes the decay of the total energy with respect to time. It plays the role of friction, making the system dissipative.

Hence, the total energy is bounded by the initial energy of the system $0 \leq \mathcal{E}(t) \leq \mathcal{E}_0$ for all $t \geq 0$. This fact together with the property that $\lim_{r \rightarrow 0, \infty} \varphi(r) = \infty$ implies via (2.12) the existence of two constants $r_m > 0$ and $0 < r_M < \infty$, dependent on N , such that

$$0 < r_m \leq |x_i(t) - x_j(t)| \leq r_M, \quad \forall i, j \in \{1, \dots, N\}, \quad \forall t \geq 0, \quad (2.14)$$

which means we have aggregation and absence of collisions. The globality of the solution is then a simple consequence.

Finally, what remains to show is that $\lim_{t \rightarrow \infty} \mathcal{A}(t) = 0$. This shall be done by showing that the kinetic energy satisfies $\mathcal{K}(t) \rightarrow_{t \rightarrow \infty} 0$, hence leading to $v_i(t) \rightarrow_{t \rightarrow \infty} 0$ for each $i = 1, \dots, N$ and thus $\lim_{t \rightarrow \infty} \mathcal{A}(t) = 0$. The fact that $\psi_b(r) > 0$ and $\psi'_b(r) < 0$ for all $r > 0$ leads to

$$\frac{d\mathcal{E}}{dt}(t) \leq -\frac{\psi_b(r_M)}{2N} \sum_{i=1}^N \sum_{j=1, j \neq i}^N |v_j(t) - v_i(t)|^2 = -\psi_b(r_M) \sum_{i=1}^N |v_i(t)|^2 = -c_\star \mathcal{K}(t),$$

with $c_\star := 2\psi_b(r_M)$, thus

$$c_\star \int_0^\infty \mathcal{K}(s) ds \leq \mathcal{E}_0. \quad (2.15)$$

This means the kinetic energy $\mathcal{K}(t)$ is integrable. To show that it converges towards zero at infinity, one shows that it is uniformly continuous. Indeed, remark that

$$\frac{d\mathcal{K}}{dt} = -\frac{1}{2N} \sum_{i=1}^N \sum_{j=1, j \neq i}^N \psi_b(r_{ij}) |v_j(t) - v_i(t)|^2 - \frac{1}{2N} \sum_{i=1}^N \sum_{j=1, j \neq i}^N \frac{\varphi'_s(r_{ij})}{r_{ij}} (x_i(t) - x_j(t), v_i(t) - v_j(t)),$$

with the first term on the right hand side being integrable (see (2.13)) and the last term bounded in time (see (2.14) and (2.12)). This permits via integration to show that $\mathcal{K}(t)$ is uniformly continuous and we finished the proof. \blacksquare

We would like to conclude this chapter with some comments about the exponential decay rate of the solution towards the equilibrium configuration. This property is very useful in practical applications, as it permits to estimate (if the constants are known) how far one is from the equilibrium, and in particular to estimate the convergence rate.

To investigate the exponential decay rate of the velocities towards zero, we need to introduce some notation. The equilibrium solutions are denoted by $(x_i^{eq}, v_i^{eq})_{i=1}^N$ and satisfy $v_i^{eq} = 0$ as well as $\sum_{j=1, j \neq i}^N \nabla_{x_i} [\varphi(|x_i^{eq} - x_j^{eq}|)] = 0$ for all $i = 1, \dots, N$; the equilibrium distances between the particles will be denoted by $r_{ij}^{eq} := |x_i^{eq} - x_j^{eq}|$, the equilibrium energy \mathcal{E}_{eq} is then given by

$$\mathcal{E}_{eq} := \frac{1}{2N} \sum_{i=1}^N \sum_{j=1, j \neq i}^N \varphi(r_{ij}^{eq}), \quad 0 \leq \mathcal{E}_{eq} \leq \mathcal{E}_0,$$

and finally let us introduce the quantity $\tilde{\mathcal{E}} := \mathcal{E} - \mathcal{E}_{eq}$, which shall decrease towards zero, when the equilibrium is approached. Furthermore, one needs to introduce a more adequate Lyapunov functional, as for the standard energy one only has

$$\frac{d\tilde{\mathcal{E}}}{dt}(t) = \frac{d\mathcal{E}}{dt}(t) \leq -\frac{\psi_b(r_M)}{2N} \sum_{i=1}^N \sum_{j=1, j \neq i}^N |v_j(t) - v_i(t)|^2 = -\psi_b(r_M) \sum_{i=1}^N |v_i(t)|^2 = -c_\star \mathcal{K}(t).$$

This inequality shows that the total energy stops decreasing for $\mathcal{K}(t) = 0$, however it does not show that the total energy tends towards zero. Ideally, in order to conclude via Gronwall's inequality, we would need an inequality of the type $\frac{d\tilde{\mathcal{E}}}{dt}(t) \leq -c\tilde{\mathcal{E}}(t)$, with some $c > 0$, however in our case the potential energy is missing on the right hand side. We shall thus proceed with hypocoercivity arguments to restore the full Lyapunov functional on the right hand side. For this one can consider the following new functional \mathcal{G} with corrector term χ

$$\mathcal{G}(t) := \mathcal{E}(t) + \alpha\chi(t), \quad \chi(t) := \frac{1}{N} \sum_{i=1}^N \sum_{j \neq i}^N \frac{\varphi'(r_{ij})}{r_{ij}} (x_i(t) - x_j(t), v_i(t) - v_j(t)),$$

with a constant $\alpha > 0$ to be chosen such that \mathcal{G} is indeed a Lyapunov functional corresponding to the system (2.11). The procedure is the following: show first that there exist some constants $c_m, c_M > 0$ such that along the trajectories of system (2.11) one has a sort of equivalence such as $c_m \tilde{\mathcal{E}}(t) \leq \tilde{\mathcal{G}}(t) \leq c_M \tilde{\mathcal{E}}(t)$, and then show that $\frac{d\tilde{\mathcal{G}}}{dt}(t) \leq -c \tilde{\mathcal{G}}(t)$. This would allow to prove the exponential decay rate in the \mathcal{G} -entropy sense, the full proof is however for the moment still an unsolved problem in the general framework.

In the simplified case of two drones however, we were able to perform the above mentioned steps, and to conclude the exponential decay rate proof. The following lemma states this result.

Lemma 2.5.1 *Let us consider the situation of 2 drones ($N = 2$) with position and velocity $(x_i(t), v_i(t))_{i=1}^2 \in \mathbb{R}^d \times \mathbb{R}^d$ and denote the differences by $x(t) := x_1(t) - x_2(t)$ and $v(t) := v_1(t) - v_2(t)$. The three zone model describing the dynamics of these two drones writes under the form of the following ODE system*

$$\begin{cases} x'(t) = v(t) \\ v'(t) = -\psi v(t) - \theta(|x(t)|) x(t) \end{cases}, \quad \forall t \in \mathbb{R}^+, \quad (2.16)$$

where we denoted $\theta(r) := \frac{\varphi'(r)}{r}$ for $r > 0$. To simplify we assumed that the alignment strength $\psi > 0$ is a constant and the unbounded attraction/repulsion potential φ satisfies besides (9) also the property

$$0 \leq c_1 \varphi(r) \leq [\varphi'(r)]^2 \leq c_2 \varphi(r), \quad \forall r \geq r_m > 0, \quad (2.17)$$

for some $c_1, c_2 > 0$, and where $r_m > 0$ is the minimal distance between the particles during the dynamics (see Thm. 0.4.5). Under these conditions the velocity $v(t)$ decays in the long time limit $t \rightarrow \infty$ exponentially fast towards $v_c \equiv 0$.

Let us remark here that a potential φ satisfying (2.17) is for example

$$\varphi(r) := \frac{r^2}{2} + \frac{1}{r} - \frac{3}{2}, \quad \forall r > 0.$$

Proof: Firstly we observe that we are in the framework of Theorem 0.4.5, hence there exist a unique global solution for our problem (2.16), with a flocking behaviour in the long-time limit. The total energy of the system as well as the modified Lyapunov functional are given by

$$\mathcal{E}(t) := \frac{1}{2}|v(t)|^2 + \varphi(r(t)), \quad \mathcal{G}(t) := \mathcal{E}(t) + \alpha \varphi'(r(t)) \frac{x(t) \cdot v(t)}{r(t)}, \quad r(t) := |x(t)|,$$

with the constant $\alpha > 0$ to be adequately fixed. The equilibrium solutions to (2.16) are given by (x^{eq}, v^{eq}) such that $v^{eq} \equiv 0$ and $\theta(r^{eq}) \equiv 0$, with $r^{eq} := |x^{eq}|$, hence $\mathcal{E}_{eq} \equiv 0$ in this case ($\varphi'(r^{eq}) = \varphi(r^{eq}) = 0$).

We observe then that

$$\frac{d\mathcal{E}}{dt}(t) = -\psi |v(t)|^2 \leq 0, \quad (2.18)$$

but this is not enough to get the exponential decay of $\mathcal{E}(t)$. However for the modified functional \mathcal{G} we have

$$\frac{d\mathcal{G}}{dt}(t) = -\psi |v(t)|^2 + \alpha \frac{\theta'(r)}{r(t)} (x(t) \cdot v(t))^2 + \alpha \theta(r(t)) |v(t)|^2 - \alpha \theta^2(r) |x(t)|^2 - \alpha \psi \theta x(t) \cdot v(t).$$

The equivalence between $\mathcal{G}(t)$ and $\mathcal{E}(t)$, meaning the existence of two constants $c_m, c_M > 0$ such that $c_m \mathcal{E}(t) \leq \mathcal{G}(t) \leq c_M \mathcal{E}(t)$, is a simple consequence of the assumption (2.17) and the fact that we have flocking. The second inequality to be shown, namely $\frac{d\mathcal{G}}{dt}(t) \leq -c_\star \mathcal{G}(t)$, is a consequence of the flocking, meaning the swarm evolves in a bounded region and in particular that one has $0 < r_m \leq r(t) \leq r_M$, as well as of the fact that the velocities tend towards v_c in the long-time limit. However, to get this last inequality of strictly decreasing entropy, the obtained constant $c_\star > 0$ can be very small, which yields a slow (pessimistic) exponential decay rate.

On Figure 2.1 we plotted, as an example, the corresponding evolutions of $\mathcal{E}(t)$ as well as of $\mathcal{G}(t)$. One observes firstly that the energy $\mathcal{E}(t)$ is slightly oscillating, with $\mathcal{E}'(t) = 0$ where the velocity $v(t)$ is vanishing (see (2.18)), and $\mathcal{E}(t)$ seems to have in “average” an exponential decay. To compare, we plotted in addition to this curve the modified Lyapunov functional $\mathcal{G}(t)$, which shows a nicer exponential decay, however still not a perfect one. Indeed, the oscillations are somehow damped a little bit, and more importantly one can observe that $\mathcal{G}(t)$ is now strictly decreasing, its slope remaining far from zero (in finite time), while $\mathcal{E}'(t)$ vanishes. This is due to the additional correction term, which continues to dissipate (the entropy) even if $v(t) = 0$.

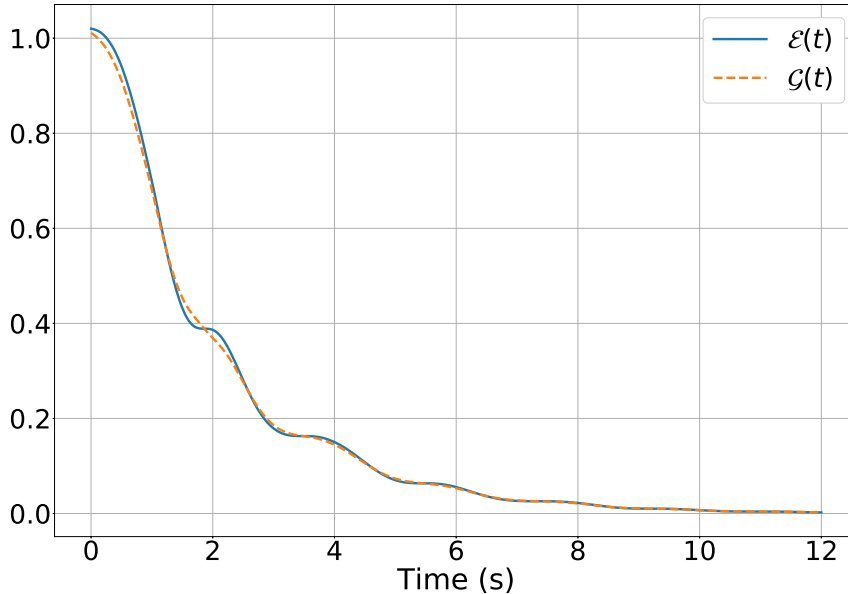


Figure 2.1: Time evolution of $\mathcal{E}(t)$ as well as of $\mathcal{G}(t)$ corresponding to system (2.16).

Chapter 3

Drone swarm modelling and simulation

The aim of this chapter is to expose the first insights of the drone swarm modelling and its specificities, as well as to present some first numerical simulations. Remark that we are particularly interested in the long-time behaviour of a large swarm of drones ($N \geq 1$).

Let us fix now our three-zone model for the description of the dynamics of a swarm of N drones. The evolution of each agent, with position and velocity $(x_i, v_i) \in \mathbb{R}^d \times \mathbb{R}^d$, is governed as usual by Newton's laws of classical mechanics, which read for all $t \geq 0$

$$\begin{cases} x'_i(t) = v_i(t), \\ v'_i(t) = \gamma \sum_{j=1}^N \psi(|x_i - x_j|) (v_j - v_i) - \gamma \sum_{j=1, j \neq i}^N \nabla_{x_i} [\varphi(|x_i - x_j|)], \end{cases} \quad \forall i = 1, \dots, N, \quad (3.1)$$

where γ is either 1 or $1/N$. The scaling $\gamma = 1/N$ of the force is only needed for the large-swarm limit $N \rightarrow \infty$, for getting a mesoscopic (kinetic) description. Otherwise one can take $\gamma = 1$. The communication weight $\psi_{ij} := \psi(|x_i - x_j|)$ shall satisfy the following assumptions

$$\psi \in C^1(\mathbb{R}_*^+), \quad \psi(r) > 0 \text{ and } \psi'(r) \leq 0 \quad \forall r > 0.$$

In particular we shall choose a singular communication weight in zero, namely

$$\psi(r) := \frac{\alpha}{r^\beta}, \quad \alpha > 0, \beta \geq 0, \forall r \in \mathbb{R}^+.$$

Concerning the potential φ , it contains the repulsion and attraction part, and we shall assume that $\varphi \in C^1(\mathbb{R}_*^+)$ is of potential-well type, bounded from below. For instance, one may take a quadratic potential (bounded repulsion)

$$\varphi(r) := \frac{1}{2}(r - \eta)^2, \quad \eta > 0, \forall r \in \mathbb{R}^+,$$

or a potential with singular repulsion as for example

$$\varphi(r) := \frac{r^2}{2} + \frac{1}{r} - \frac{3}{2}, \quad \forall r \in \mathbb{R}^+,$$

or even decouple the attraction and repulsion forces as in the more general form

$$\varphi(r) := \frac{F_A}{q} (r - \eta_A)_-^q + \frac{F_R}{p} (r - \eta_R)_+^p,$$

with positive constants $p, q, F_A, F_R, \eta_A, \eta_R$ to be chosen in such a manner to get the desired swarm configuration. To give only an example, we plotted in Fig. 3.1 a possible potential choice.

One delicate task in drone swarm modelling is now the exploration of the different stationary configurations one may obtain in the long-time limit $t \rightarrow \infty$ for large drone populations $N \gg 1$, and this by varying the shapes of the attraction/repulsion potentials. These investigations are of particular interest for the obtention of stable and realistic swarm configurations. Later on we shall also introduce some other specific physical effects, such as obstacles, a target, time-delays and self-propulsion.

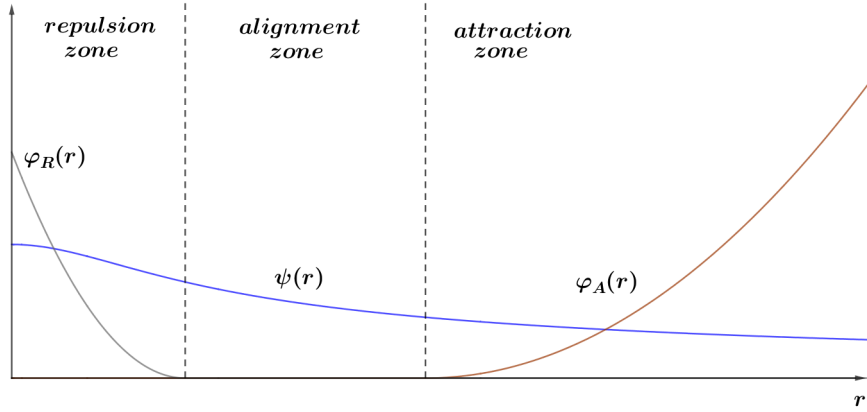


Figure 3.1: Example of attraction, alignment and repulsion potentials (bounded in $r = 0$) for the 3zone model.

3.1 Some equilibrium configurations

The main objective is now to understand which choice of the attraction/repulsion and alignment kernels give rise to the desired drone configuration (for large $N \gg 1$) in terms of inter-drone spacings, realistic drone velocities and stable steady states. Let us remark, that once the drones move with constant velocities, the shape of the pattern is given by the balance of the repulsive resp. attractive forces acting on each drone, namely by the formula

$$\sum_{j=1, j \neq i}^N \nabla_{x_i} [\varphi(|x_i - x_j|)] = 0, \quad \forall i = 1, \dots, N.$$

Note that these particular solutions are not equilibria in the classical sense, meaning we do not necessarily have $x'_i(t) = v'_i(t) \equiv 0$ for all i . Here, we are dealing with solutions with particular properties. For instance, flocking solutions describe configurations with particles moving with uniform speeds $v_i(t) \equiv v_c$ and corresponding positions

$$x_i(t) = x_i^0 + v_c t.$$

Many different types of pattern (asymptotic configurations) emerge in the long-time limit $t \rightarrow \infty$, regulated by the relative strength of the repulsion/attraction potentials, some of them are stable, other unstable, and not all of them are of interest in our case. To give only some examples, we plotted in Figures 3.2-3.4 annular formations, uniform discs or ring-formations, and their corresponding potentials $\varphi_{ann}(r) := (r - 5)^2$ as well as

$$\varphi_{cris}(r) := \begin{cases} 10(r - 5)^2, & 0 \leq r \leq 5 \\ \frac{1}{3}(r - 5)^2, & 5 \leq r \leq 6 \\ 1 - \frac{2}{3(r-5)}, & r \geq 6 \end{cases}, \quad \varphi_{ring}(r) := \begin{cases} \frac{1}{10}(r - 5)^2, & 0 \leq r \leq 5 \\ \frac{1}{3}(r - 5)^2, & 5 \leq r \leq 6 \\ 1 - \frac{2}{3(r-5)}, & r \geq 6 \end{cases}.$$

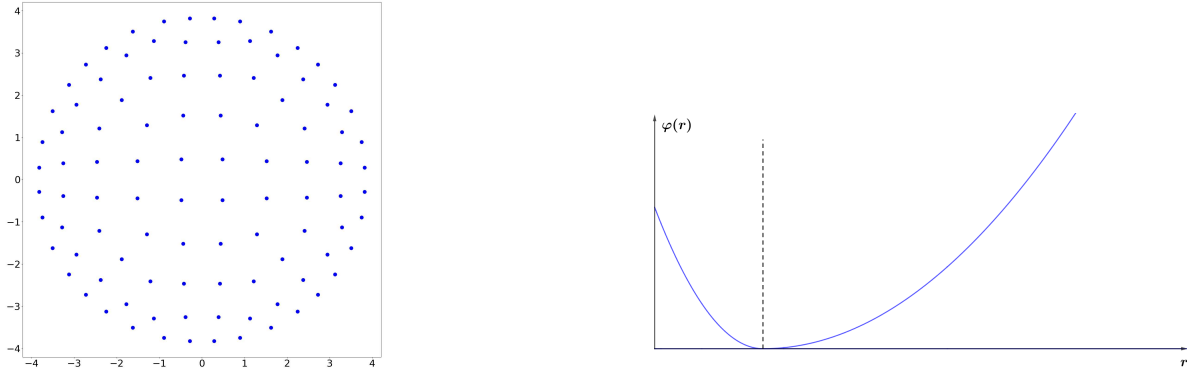


Figure 3.2: Annular formation for a potential $\varphi_{ann}(r) := (r - 5)^2$.

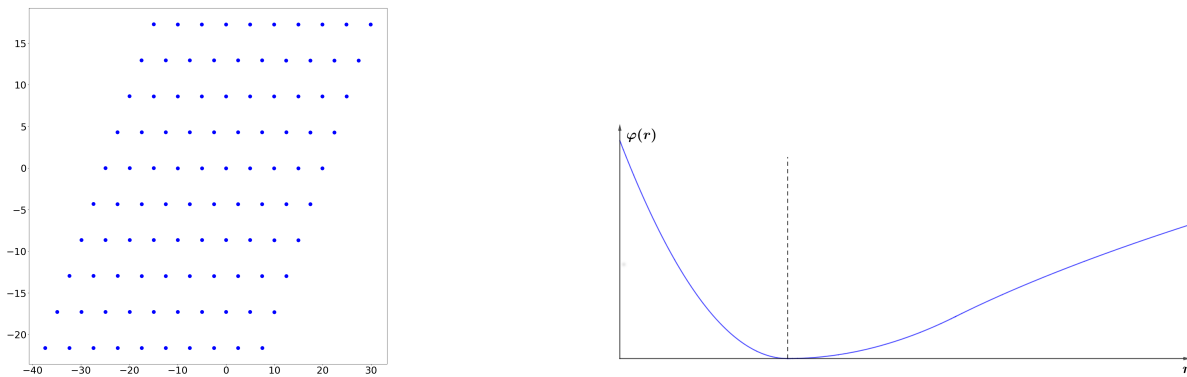


Figure 3.3: Uniform disc formation for the potential $\varphi_{cris}(r)$.

Properties like radius of the cloud, particle density and accumulation to the border change with increasing N . What can be observed is that if one chooses stronger and stronger repulsive potentials at the origin, the cloud of the particles gets larger and larger with increasing N , whereas milder repulsive potentials lead to clustering when

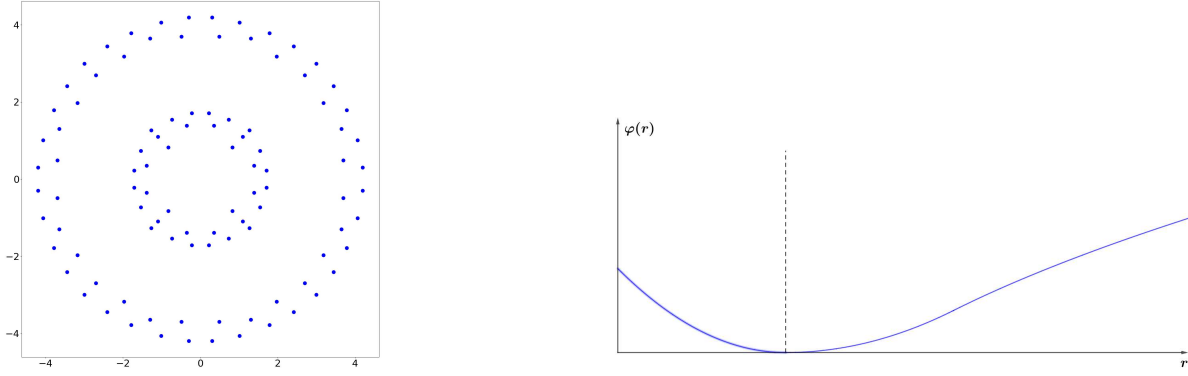


Figure 3.4: Ring formation for a potential $\varphi_{ring}(r)$.

increasing the number of drones N . The effect of strong attraction potentials is the formation of a bounded cloud, leading to a ring with increasing number of particles.

To illustrate some effects, let us investigate what happens with the cloud when taking the quadratic potential $\varphi(r) = \frac{1}{2}(r - \eta)^2$, with $\eta > 0$. At equilibrium one has

$$\begin{aligned}
 0 &= \sum_{j=1, j \neq i}^N \frac{(r_{ij} - \eta)}{r_{ij}} (x_j - x_i) \\
 &= \sum_{j=1}^N (x_j - x_i) - \eta \sum_{j=1, j \neq i}^N \frac{x_j - x_i}{r_{ij}} \\
 &= N(x_{mean} - x_i) - \eta \sum_{j=1, j \neq i}^N \frac{x_j - x_i}{r_{ij}}.
 \end{aligned}$$

This yields

$$N|x_i - x_{mean}| = \eta \left| \sum_{j=1, j \neq i}^N \frac{x_j - x_i}{r_{ij}} \right| \leq N\eta,$$

implying

$$\sup_{i \in [1, N]} |x_i - x_{mean}| \leq \eta.$$

This means that at equilibrium all drones are contained in a sphere of radius η centered in the center of mass of the fleet. Furthermore observe that this inequality does not depend on the amount of drones N . As a consequence, if one adds more and more drones with the same parameters, the drone swarm will not blow up, but the drones will rather concentrate in that sphere, as illustrated on Fig. 3.5.

To study these different pattern formations, some characteristic properties to look for are the time-evolution of the minimal resp. maximal inter-drones distances, and their dependence on N , *i.e.*

$$d_{min}(t) := \min_{i \neq j} |x_i(t) - x_j(t)|, \quad d_{max}(t) := \max_{i \neq j} |x_i(t) - x_j(t)|.$$

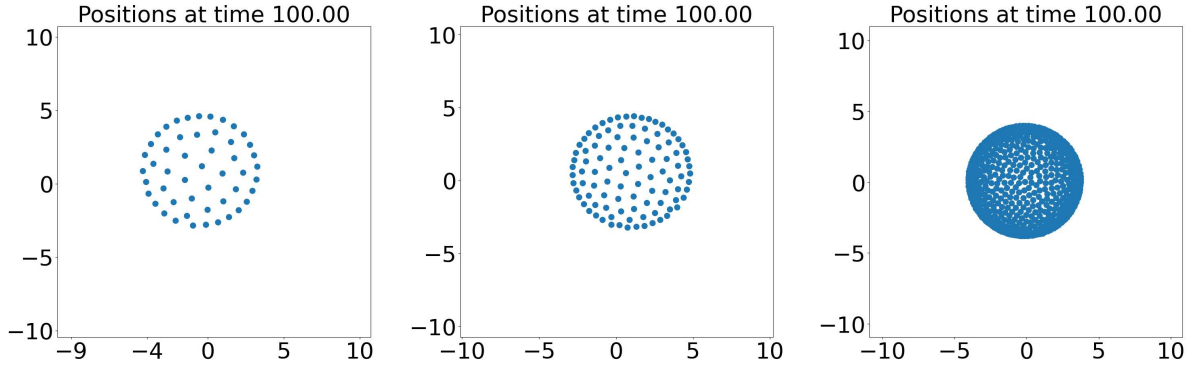


Figure 3.5: Examples of swarm configurations for a quadratic potential $\varphi(r) = \frac{1}{2}(r - \eta)^2$ and different drone numbers $N = 50, 100, 500$.

3.2 Specificities of drone swarms and other physical effects

When dealing with the modelling of drone swarms, one has to face particular problems, as for example:

- **Force/power constraints:** Drones are powered by motors, which have their own, particular characteristics, yielding a maximal force strength and a maximal power, which cannot be surpassed;
- **Reactivity constraints:** Drones need time to receive and process the information (like positions and velocities) from other drones, and to transmit their own information. This necessarily leads to time delays in the reactivity of the drones;
- **Energy constraints:** Energy is a substantial and rare resource and thus its wise employment is of paramount importance for the drone swarm lifetime and the desired mission success;
- **Connectivity:** Maintaining stable connectivity within the drones while achieving at the same time the best area-coverage is an essential request.

Furthermore, the main goal of drone studies is to provide a model of autonomously evolving drones in a realistic setting. Thus, the model should contain as many as possible system-specific features as can be taken into account, for example in addition to the above mentioned constraints, we shall consider:

- **Obstacle avoidance** can be modelled via repulsive artificial forces, which push the drone back and prevent it from colliding with the occurring obstacles, *i.e.*

$$F_i^{obs} = -\nabla_{x_i} [\varphi_{obs}(|x_i - x_{obs}(t)|)] , \quad \varphi_{obs}(r) := \frac{1}{r^\alpha}, \quad \alpha > 0;$$

- **Destination point (target)** can be modelled by an attraction force, which helps the drone to reach the goal. Moving targets or **leaders** can be also modelled via

attraction fields, *i.e.*

$$F_i^{tar} = -\nabla_{x_i} [\varphi_{tar}(|x_i - x_{tar}(t)|)] , \quad \varphi_{tar}(r) := r^\alpha , \quad \alpha > 0 ;$$

- **Friction** with the environment is usually modelled by a force $F_i^{fric} = -\mu(v_i) v_i$. One can choose either a simple linear drag force, *i.e.* $\mu(v) := \nu$ with constant $\nu > 0$, or a nonlinear Rayleigh-Helmholtz drag, *i.e.* $\mu(v) := \beta |v|^2$ with $\beta > 0$.
- **Self-propulsion** of the agents can be modelled by adding a force of the form $F_i^{prop} = \alpha v_i$, with $\alpha > 0$ describing a constant acceleration of the particles. Normally self-propulsion and friction are modelled together via a force term $F_i^{fp}(v_i) = -(\beta |v_i|^2 - \alpha) v_i$, leading to an asymptotic velocity of magnitude $\sqrt{\alpha/\beta}$.
- **Environmental disturbances**, like for example unpredictable fluctuations in the wind, can be modelled by introducing some random force field in the model F_i^{fluc} , meaning noise terms representing the incessant impact of the environment on the drones;
- **Inner noise**, meaning the inaccuracy of the sensors that measure the positions and velocities of the drones, can also be characterized by the introduction of stochastic force fields.

So far we have treated the drones as responding to the environment they perceive, via some simple mathematical rules, yielding thus an alternating sequence of *perception* and *action*. However one can go one step further and treat the drone additionally as "learning agents", meaning between the perception of its surroundings and the action step, the drone can study in detail the situation (*deliberation step*) and adapt its response by considering the personal history of interactions and the feedback he got.

Combining several of the previously discussed effects leads to rich mathematical behaviours. For instance the competition between the Rayleigh-Helmholtz friction and the self-propulsion leads to an asymptotic velocity of magnitude $\sqrt{\alpha/\beta}$ in the long-time limit. The nonlinearity leads also to very nice mathematical questions, as for example the occurrence of phase-transitions if noise is added to the system. In some words, phase-transition is a process during which a system, constituted of a large number of particles, undergoes a transition between two different "phases" of the system, for example from an ordered towards a disordered phase, defined by a specific parameter, as for ex. an order parameter. Such phase-transitions are frequently observed for example in bird-swarm dynamics, see Fig. 3.6.

The study of phase transitions is a very active research area. Let us cite a few examples of phase transition phenomena, occurring in collective models for various reasons.

Firstly, in continuous versions of the Vicsek model with noise, the behaviour of the system is locally related to the density of the agents. More specifically, in regions where the spatial density of the agents is high enough (higher than a given explicit threshold), meaning the agents are able to communicate, their velocity align and the dynamics of their spatial density is accurately described by a fluid system of equations. In regions where the distribution of agents is lower than that threshold, however, these agents are

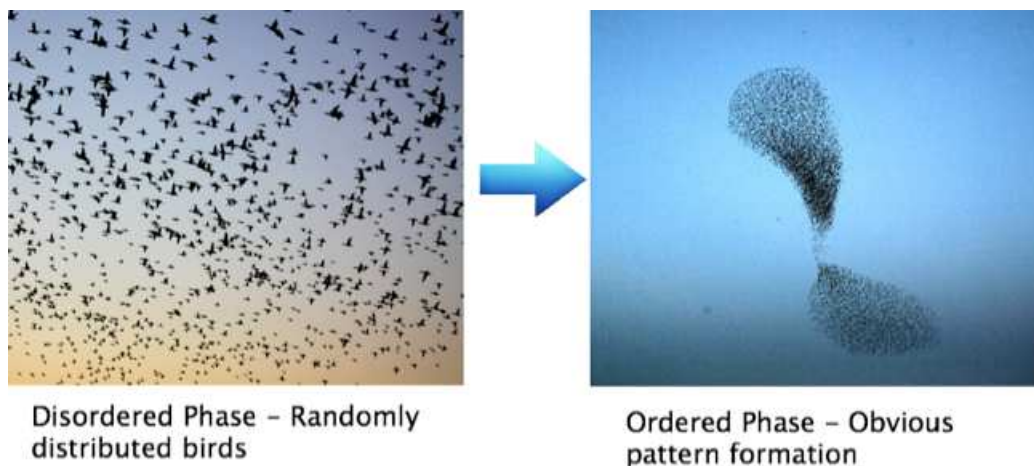


Figure 3.6: Examples of phase-transition in a bird swarm [47].

unable to efficiently communicate, their velocity becomes uniformly distributed on the sphere, and their spatial density follows a diffusion-type equation. Such a discussion can be found in [20].

Another example of phase-transition occurs in the Kuramoto model, given in (11), whose solutions change their behaviour when varying the strength of the communication rate K . There exists a threshold K_c such that, if $K < K_c$ one gets in the long-time asymptotics a uniform distribution of oscillators. However, when $K > K_c$ the oscillators begin to automatically synchronise over time. This is called "phase-locking". One can refer to [26] for more detailed discussions on the subject.

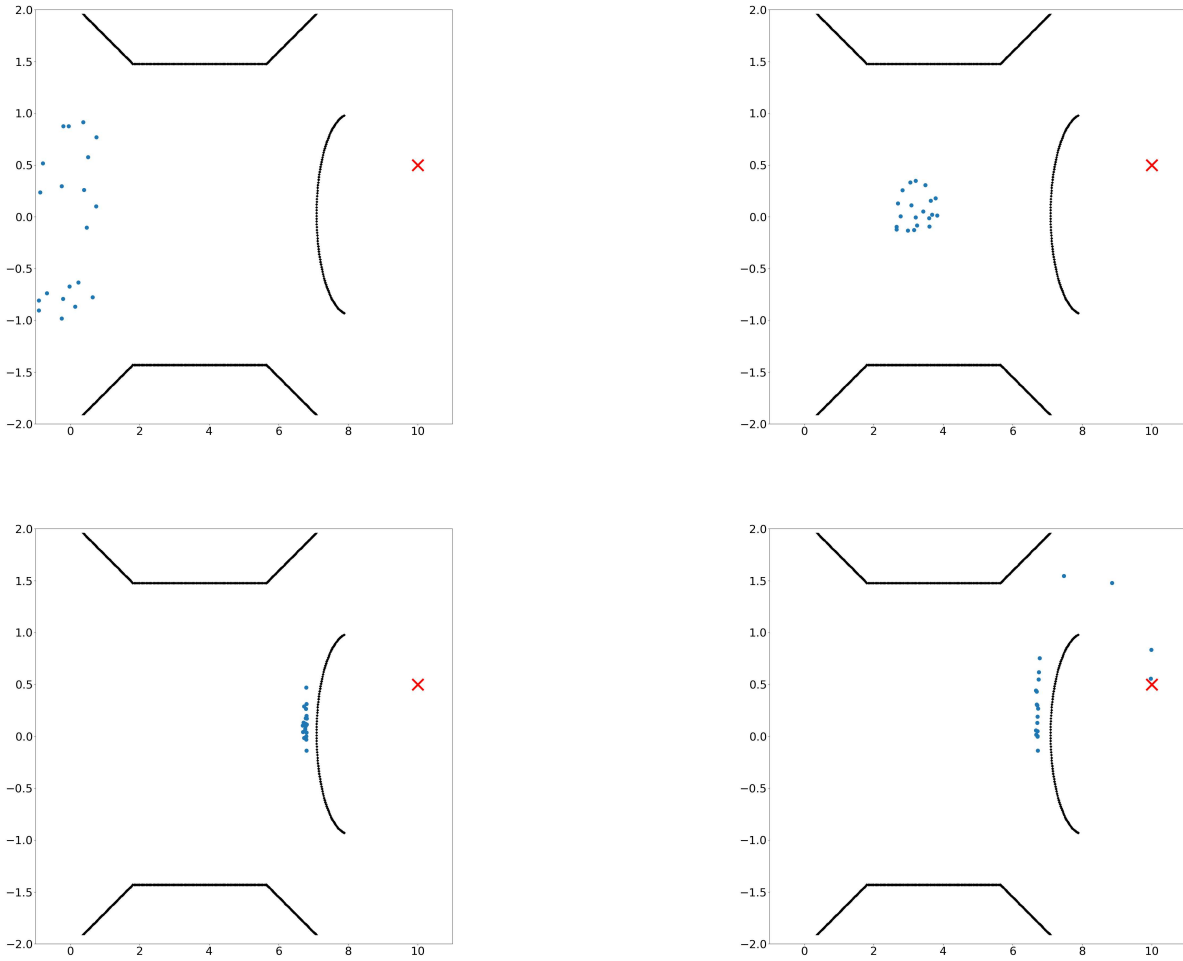
Let us finish this discussion by presenting some simulations in Figure 3.7 corresponding to a swarm of $N = 20$ drones, whose dynamics is governed by a three-zone model with additional terms representing noise, friction, some obstacles and a target (see model (3.2)). The parameters and functions chosen for this simulations are

$$\varphi(r) := \frac{(r-1)^2}{2}, \quad \psi(r) := \frac{1}{r}, \quad \gamma = 1.$$

The numerical simulations have been performed with a fourth-order Runge-Kutta scheme (RK4). One observes very nicely on these figures the different repulsion and attraction forces. Noise can be also discerned by the fact that the drone density does not form a homogeneous cloud.

3.3 Mesoscopic and macroscopic descriptions

Several numerical difficulties arise when trying to solve (3.1), related for example to long-time studies, nonlinearities, delicate competition between rather different terms, multi-scale nature of the problem *etc.* One of these difficulties is linked to the large number of drones $N \gg 1$ one is simulating, leading to very large coupled systems. Sometimes to get a rapid first insight of how a drone swarm evolves in time, given an initial



drone distribution, one can move towards mesoscopic or even macroscopic approaches, which are numerically more attractive but poorer from a physical point of view. Indeed, these meso/macroscopic models do not follow the precise trajectories of each agent, but deal with averaged distribution quantities, like drone space-velocity distribution functions $f(t, x, v)$ or even more macroscopically like drone densities $n(t, x)$, drone mean velocities $u(t, x)$, total energy densities $\mathcal{E}(t, x)$ *etc.* To recover these meso/macroscopic models from the underlying particle models, asymptotic limits have to be considered, letting the number of drones N tend towards infinity.

3.3.1 Kinetic descriptions

On the way towards a macroscopic drone model, one departs from a mesoscopic description of a drone swarm, which provides the evolution of the particle distribution function $f(t, x, v)$ in the phase space $\mathbb{R}^d \times \mathbb{R}^d$. Such a mesoscopic description is obtained starting for example from the following, underlying particle model, including apart of the usual alignment, repulsion and attraction terms, also other specific features such as a target

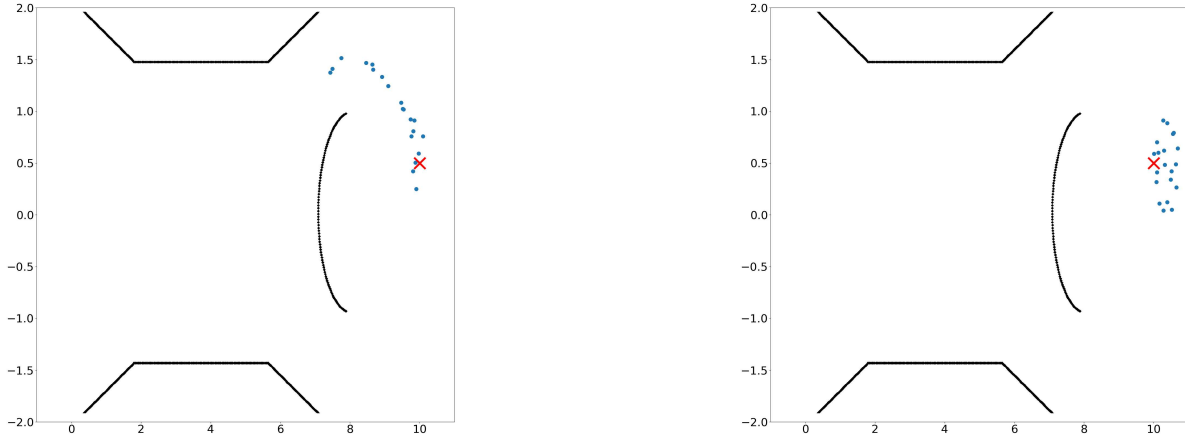


Figure 3.7: Time evolution of a swarm of $N = 50$ drones starting on the left of the simulation domain and converging towards a target (red point), by avoiding obstacles on their way.

for the swarm (destination point), friction as well as noise, *i.e.*

$$\begin{cases} x'_i(t) = v_i(t), \\ v'_i(t) = -\gamma v_i(t) - (\nabla_x V)(x_i(t)) + \frac{1}{N} \sum_{j=1}^N \psi_{ij} (v_j - v_i) - \frac{1}{N} \sum_{j=1, j \neq i}^N (\nabla_x \varphi)(x_i - x_j) + \eta(t). \end{cases} \quad (3.2)$$

A mean-field limit permits then to obtain the corresponding kinetic model

$$\partial_t f + v \cdot \nabla_x f - \nabla_v \cdot [(\gamma v + \nabla_x V + \nabla_x \varphi \star n) f] + \nabla_v \cdot [F_a(f) f] = \sigma \Delta_v f, \quad (3.3)$$

where $f(t, x, v) dx dv$ represents the probability to find at instant t a drone in the volume $dx dv$ around the phase-space point (x, v) . Here we denoted the drone density as well as the averaged velocity alignment force by

$$n(t, x) := \int_{\mathbb{R}^d} f(t, x, v) dv, \quad F_a(f)(t, x, v) := \int_{\mathbb{R}^d} \int_{\mathbb{R}^d} \psi(x-y) (w-v) f(t, y, w) dy dw.$$

Furthermore $\eta(t)$ is a Gaussian white noise with $\sigma > 0$ the noise strength, $\gamma > 0$ is here the friction coefficient and the potential V is modelling an exterior attraction force towards a given target. Let us observe that the collision operator of the RHS conserves the mass, but neither the momentum nor the energy.

The formal passage from the particle model (3.2) towards the kinetic model (3.3) can be understood (as nicely explained in [15]) via the introduction of an empirical measure

$$\mu_t^N(x, v) := \frac{1}{N} \sum_{i=1}^N \delta_{(x_i(t), v_i(t))}, \quad (3.4)$$

which makes the link between the two descriptions. Indeed, under suitable assumptions one can show that (3.2) admits a global-in-time smooth solution, and that under these

conditions the measure (3.4) satisfies the kinetic equation (3.3) in a distributional sense.

To give only an idea of this formal proof, take $\theta \in C_c^1(\mathbb{R}^d \times \mathbb{R}^d)$ and compute

$$\begin{aligned} \frac{d}{dt} \int_{\mathbb{R}^d \times \mathbb{R}^d} \theta(x, v) \mu_t^N(dx dv) &= \frac{d}{dt} \left(\frac{1}{N} \sum_{i=1}^N \theta(x_i(t), v_i(t)) \right) \\ &= \frac{1}{N} \sum_{i=1}^N [\nabla_x \theta(x_i(t), v_i(t)) \cdot v_i(t) + \nabla_v \theta(x_i(t), v_i(t)) \cdot v_i'(t)]. \end{aligned}$$

Remarking that (if one skips the noise here)

$$\begin{aligned} v_i'(t) &= -\gamma v_i(t) - \nabla_x V(x_i(t)) - \int_{\mathbb{R}^d \times \mathbb{R}^d} \psi(x_i(t) - y) (w - v_i(t)) \mu_t^N(dy dw) \\ &\quad - \int_{\mathbb{R}^d \times \mathbb{R}^d} (\nabla_x \varphi)(x_i(t) - y) \mu_t^N(dy dw). \end{aligned}$$

and inserting this last equality in the above formula, permits to prove that μ_t^N is a distributional solution of the kinetic equation (3.3). We refer the interested reader to [7,15,30] for more rigorous mean-field limit studies.

Let us finally mention that, to be closer to reality one can couple the particle or kinetic drone-model with a fluid model which describes the environment in which the agents evolve. The coupling is done by means of the so-called Stokes drag force $F_d(t, x, v) = \xi(t, x) - v$. To be more precise, the drone evolution can be described via the following kinetic equation

$$\partial_t f + v \cdot \nabla_x f - [\nabla_x V + (\nabla_x \varphi) \star n] \cdot \nabla_v f = \nabla_v \cdot [(v - \xi) f - F_a(f) f + \sigma \nabla_v f], \quad (3.5)$$

coupled to a viscous, compressible Navier-Stokes fluid model for the description of the environment variables (ρ, ξ)

$$\begin{cases} \partial_t \rho + \nabla_x \cdot (\rho \xi) = 0, \\ \partial_t (\rho \xi) + \nabla_x \cdot (\rho \xi \otimes \xi) + \nabla_x p(\rho) + L \xi = \int_{\mathbb{R}^d} (v - \xi) f dv, \end{cases} \quad (3.6)$$

with the pressure and the Lamé operator given by

$$p(\rho) := \rho^\alpha, \quad \alpha > 1; \quad L \xi := -\mu \Delta_x \xi - \mu' \nabla_x [\nabla_x \cdot \xi], \quad \mu > 0, \quad \mu + \mu' > 0.$$

In some situations (for example when the fluid is a gas), one can consider the background density as constant, leading thus to the incompressible Navier-Stokes model. Furthermore, one can assume that the fluid (ρ, ξ) interacts only with itself, and is hence not affected by the kinetic part, as a consequence of a sparseness assumption on the kinetic species.

3.3.2 Fluid descriptions

The numerical simulation of a kinetic equation of the type (3.3) is very costly ($6D$ in the phase-space (x, v)), such that it could be interesting to derive the corresponding fluid drone model in order to reduce complexity. Introducing now the macroscopic (mean) velocity by

$$(nu)(t, x) := \int_{\mathbb{R}^d} v f(t, x, v) dv, \quad (3.7)$$

as well as the energy and the temperature via

$$w(t, x) := \frac{1}{2} \int_{\mathbb{R}^d} |v|^2 f(t, x, v) dv = \frac{1}{2} n |u|^2 + \frac{d}{2} nT, \quad \frac{d}{2} nT := \frac{1}{2} \int_{\mathbb{R}^d} |v - u|^2 f dv,$$

and taking the moments of the kinetic equation (3.2), yields the corresponding fluid model

$$\left\{ \begin{array}{l} \partial_t n + \nabla_x \cdot (nu) = 0, \\ \partial_t (nu) + \nabla_x \cdot (nu \otimes u) + n [\nabla_x V + (\nabla_x \varphi) \star n] + \nabla_x \cdot \mathbb{P} \\ \quad = -\gamma n u - \int_{\mathbb{R}^d} \psi(x - y) n(t, y) n(t, x) [u(t, x) - u(t, y)] dy \\ \partial_t w + \nabla_x \cdot (w u + \mathbb{P} u + \mathbf{q}) + nu [\nabla_x V + (\nabla_x \varphi) \star n] \\ \quad = -2\gamma w + \sigma n - d nT (\psi \star n) - n [\psi \star (nu)] \\ \quad \quad - \int_{\mathbb{R}^d} \psi(x - y) n(t, y) n(t, x) [u(t, x) - u(t, y)]^2 dy, \end{array} \right. \quad (3.8)$$

where we denoted by \mathbb{P} and \mathbf{q} the pressure tensor and the heat flux, given by

$$\mathbb{P}(t, x) := \int_{\mathbb{R}^d} (v - u) \otimes (v - u) f(t, x, v) dv, \quad \mathbf{q}(t, x) := \frac{1}{2} \int_{\mathbb{R}^d} (v - u) |v - u|^2 f dv.$$

This fluid model is not closed. To get a self-consistent model one needs to express the pressure tensor \mathbb{P} and the heat flux \mathbf{q} by means of the unknowns (n, u, w) . This can be done either via empirical laws or by performing a physical scaling of the kinetic model (3.3), identifying a small parameter $\varepsilon \in (0, 1)$, which represents the regime of interest, and performing then an asymptotic (hydrodynamic) study, which leads finally to the corresponding (closed) fluid model for vanishing ε . The parameter ε serves as connection between the kinetic and the fluid world.

This classical (rigorous) procedure is still an open research topic in the model-case we are studying in this work. Formally the fluid limit can be obtained by assuming a mono-kinetic form of the distribution function

$$f_M(t, x, v) := n(t, x) \delta_{u(t, x)}(v), \quad (3.9)$$

where the particle density $n(t, x)$ and the average velocity $u(t, x)$ are now solutions of

the pressureless Euler equations

$$\begin{cases} \partial_t n + \nabla_x \cdot (nu) = 0, \\ \partial_t(nu) + \nabla_x \cdot (nu \otimes u) + n [\nabla_x V + (\nabla_x \varphi) \star n] \\ \qquad \qquad \qquad = -\gamma n u - \int_{\mathbb{R}^d} \psi(x-y) n(t,y) n(t,x) [u(t,x) - u(t,y)] dy. \end{cases} \quad (3.10)$$

As for the particle-kinetic passage, one can show formally that the measure valued function f_M defined in (3.9) solves the kinetic equation (3.3) in a distributional sense, as long as (n, u) satisfy the the pressureless Euler equations (3.10). This formal mono-kinetic closure leads to a vanishing pressure tensor \mathbb{P} and a vanishing heat flux \mathbf{q} , decoupling also the energy equation from the rest part of the model. More rigorous studies can be found in [1, 22, 23].

The mono-kinetic Ansatz is physically not justified, however it permits to obtain a fluid model, whose solution shows to have a rather similar behaviour as the particle model solution. To illustrate this, we present some first numerical results of a comparison between a particle drone model and the corresponding pressureless Euler model in Figures 3.8-3.9. These are preliminary results, plotted here only in order to give the reader an idea about what we are interested in, a detailed comparison is at the moment in study. The aim was to show that with lesser complexity (lower computational times and memory requirements) we can achieve with fluid simulations sufficiently satisfactory results, permitting thus to avoid the precise but time-consuming particle simulations in cases where rapid answers are needed for the coordination of drone swarms (practical aim). Naturally, if one wants to investigate more detailed physical or mathematical phenomena (fundamental aim), like instabilities, phase-transitions and so on, kinetic simulations shall be employed, and this is another subject.

The model at the basis of these simulations is the 3zone model (3.2) and the corresponding fluid model (3.8). The particle model was simulated via the standard RK4 scheme, whereas the fluid model was simulated with a standard second-order finite volume method in space and a RK2 scheme in time (see [9] for the numerical scheme). The mesh in space for the fluid simulations is rather rough ($N_x \times N_x = 50 \times 50$) to keep the complexity low and investigate the power of the fluid simulations. The time-step follows the CFL-condition. Initially all $N = 500$ drones are homogeneously distributed in a square and have all the common velocity of $v_* = (0.02, 0.02)$. What happens in time, is that the repulsion, attraction and alignment forces start to act, such that the drone swarm evolves as observed from the figures, coming nearer and nearer to an equilibrium configuration.

3.3.3 Long-time asymptotics

To complete the study of the drone-swarm modelling one interesting question is to investigate the long-time asymptotic flocking behaviour of the kinetic model (3.3) or of the corresponding fluid model (3.8), similarly to the exponential decay studies we presented for the particle model. For this, let us briefly sketch some ideas, starting from the following slightly changed kinetic equation

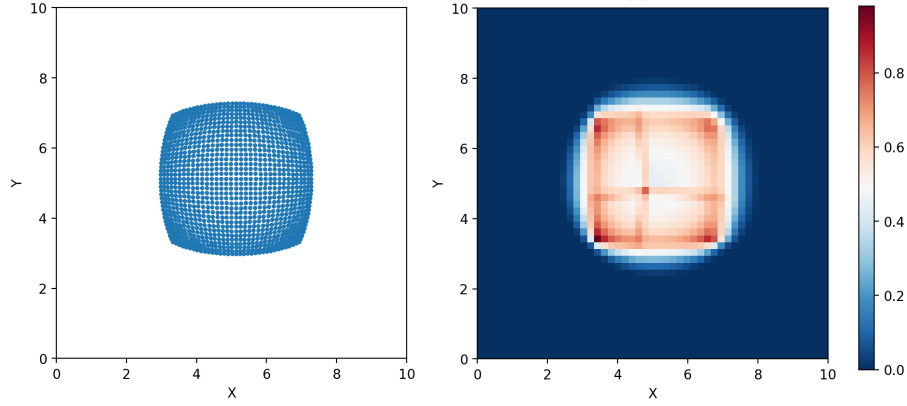


Figure 3.8: Drone swarm particle (left, $N = 500$) and fluid (right) simulations at $t = 5s$.

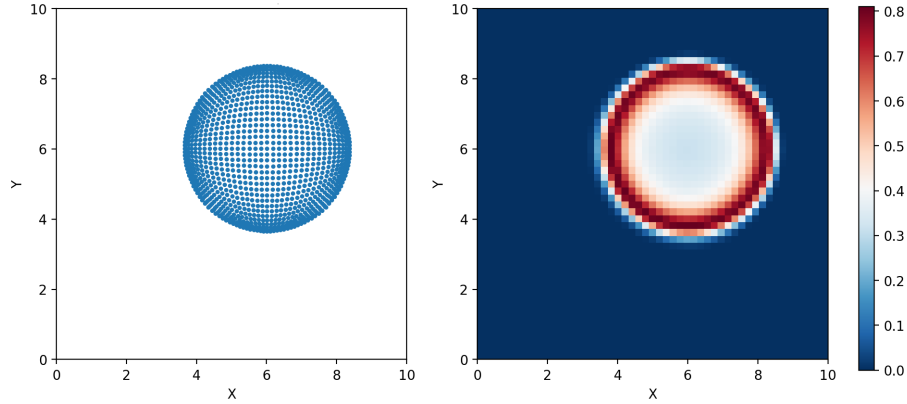


Figure 3.9: Drone swarm particle (left, $N = 500$) and fluid (right) simulations at $t = 40s$.

$$\begin{cases} \partial_t f + v \cdot \nabla_x f - [\nabla_x V + (\nabla_x U) \star n] \cdot \nabla_v f = \nabla_v \cdot [\gamma v f - G_a(f) f + \sigma \nabla_v f], \\ f(0, x, v) = f_{in}(x, v). \end{cases} \quad (3.11)$$

with the normalized alignment term given by

$$G_a(f)(t, x, v) := \frac{\int_{\mathbb{R}^d} \int_{\mathbb{R}^d} \psi(x - y) (w - v) f(t, y, w) dy dw}{\int_{\mathbb{R}^d} \int_{\mathbb{R}^d} \psi(x - y) f(t, y, w) dy dw} = \frac{\psi \star (n u)}{\psi \star n} - v =: \tilde{u} - v.$$

Remark that choosing $\psi \equiv \delta_0$ in this last formula leads to the local alignment force $G_a(f)(t, x, v) := u(t, x) - v$, where u is this time the mean velocity defined in (3.7).

Rescaling the two quantities \tilde{u} and σ as

$$\hat{u} := \frac{\tilde{u}}{\gamma + 1}, \quad \hat{\sigma} := \frac{\sigma}{\gamma + 1},$$

permits to rewrite the Fokker-Planck collision operator on the RHS of (3.11) in the more usual form

$$\mathcal{Q}(f) := (\gamma + 1) \nabla_v \cdot [(v - \hat{u}) f + \hat{\sigma} \nabla_v f] = (\gamma + 1) \nabla_v \cdot \left[\hat{\sigma} \hat{\mathcal{M}}_{\hat{u}} \nabla_v \left(\frac{f}{\hat{\mathcal{M}}_{\hat{u}}} \right) \right],$$

where we denote

$$\hat{\mathcal{M}}_0(v) := \frac{1}{(2\pi\hat{\sigma})^{d/2}} e^{-\frac{|v|^2}{2\hat{\sigma}}}, \quad \hat{\mathcal{M}}_{\hat{u}}(t, x, v) := \frac{1}{(2\pi\hat{\sigma})^{d/2}} e^{-\frac{|v - \hat{u}(t, x)|^2}{2\hat{\sigma}}}.$$

As usually, let us introduce some physical quantities corresponding to the model, like the associated free energy

$$\mathcal{G}(f)(t) := \frac{\sigma}{\gamma + 1} \int_{\mathbb{R}^d} \int_{\mathbb{R}^d} f \ln(f) dx dv + \frac{1}{2} \int_{\mathbb{R}^d} \int_{\mathbb{R}^d} f |v|^2 dx dv + \int_{\mathbb{R}^d} \left[V(x) + \frac{1}{2} (U \star n) \right] n dx, \quad (3.12)$$

which is the sum of the entropy $\mathcal{S}(t)$ (first term) and the total energy $\mathcal{E}(t)$ (last two terms). Furthermore, the dissipation term is given by

$$\mathcal{D}(f)(t) := (\gamma + 1) \int_{\mathbb{R}^d} \int_{\mathbb{R}^d} \frac{1}{f} [(v - \hat{u}) f + \hat{\sigma} \nabla_v f]^2 dx dv = \frac{\sigma^2}{\gamma + 1} \int_{\mathbb{R}^d} \int_{\mathbb{R}^d} \frac{\hat{\mathcal{M}}_{\hat{u}}^2}{f} \left[\nabla_v \left(\frac{f}{\hat{\mathcal{M}}_{\hat{u}}} \right) \right]^2 dx dv.$$

In order to get some information about the long-time asymptotics of the distribution function f , the classical procedure is to multiply the kinetic equation (3.11) by $\ln\left(\frac{f}{\hat{\mathcal{M}}_0}\right)$ and to integrate in the phase-space $dx dv$, obtaining the following evolution equation for the free energy

$$\frac{d}{dt} \mathcal{G}(t) + \mathcal{D}(f)(t) = - \int_{\mathbb{R}^d} n(t, x) u(t, x) \tilde{u}(t, x) dx + \frac{1}{\gamma + 1} \int_{\mathbb{R}^d} n(t, x) |\tilde{u}(t, x)|^2 dx,$$

which rewrites

$$\frac{d}{dt} \mathcal{G}(t) + \mathcal{D}(f)(t) + \frac{\gamma}{\gamma + 1} \int_{\mathbb{R}^d} n(t, x) |\tilde{u}(t, x)|^2 dx = - \int_{\mathbb{R}^d} n(t, x) \tilde{u}(u - \tilde{u}) dx. \quad (3.13)$$

Let us make here two observations. Firstly, in the case one has $u = \tilde{u}$, which arises for example if $\psi = \delta_0$, thus for very concentrated alignment functions, the right hand side of (3.13) vanishes. This implies then that in the long-time limit the distribution function f tends towards some function of the form $f^\infty = n^\infty(x) \hat{\mathcal{M}}_0(v)$, with zero average velocity. The zero average velocity is obtained for $\gamma > 0$. The limiting density function n^∞ is solution of the following nonlinear elliptic problem, called sometimes Poisson-Boltzmann equation

$$\frac{\sigma}{\gamma + 1} \nabla_x n^\infty = - [\nabla_x V + (\nabla_x U) \star n^\infty] n^\infty, \quad \forall x \in \mathbb{T}.$$

The second observation concerns the case with no friction, namely for $\gamma \equiv 0$. Even in this case one gets the same limit distributional function $f^\infty = n^\infty(x) \hat{\mathcal{M}}_0(v)$, with zero average velocity. Indeed this comes from the interplay between the transport and the collision operator.

All this analysis is done in the simplified case of $u = \tilde{u}$. In more general cases, with a communication weight which is concentrated around $r \sim 0$, one has to try to show the smallness of the term $u - \tilde{u}$ and to include the RHS into the LHS. Applying then standard Sobolev inequalities on (3.13) shall permit to obtain the exponential decay of f (in the entropy sense) towards the equilibrium. This problem is for the moment in study.

Chapter 4

Some fundamental inequalities

In this chapter we shall compact some classical theorems and inequalities often used in entropy methods.

4.1 Gronwall lemma

Lemma 4.1.1 (*Bellman-Gronwall lemma, integral version*)

Let $u, \varphi, \psi : [a, b) \rightarrow \mathbb{R}$ be three continuous functions on $[a, b) \subset \mathbb{R}$. Let us furthermore suppose that φ is positive on $[a, b)$ and that u satisfies the following inequality

$$u(t) \leq \psi(t) + \int_a^t \varphi(s) u(s) ds, \quad \forall t \in [a, b).$$

Then one has the estimate

$$u(t) \leq \psi(t) + \int_a^t \psi(s) \varphi(s) e^{\int_s^t \varphi(\tau) d\tau} ds, \quad \forall t \in [a, b).$$

Lemma 4.1.2 (*Gronwall lemma, integral version*)

Let $u, \varphi : [a, b) \rightarrow \mathbb{R}$ be two continuous functions on $[a, b) \subset \mathbb{R}$. Let us furthermore suppose that $\varphi \geq 0$ on $[a, b)$ and that u satisfies the following inequality, with some constant $u_0 \in \mathbb{R}$

$$u(t) \leq u_0 + \int_a^t \varphi(s) u(s) ds, \quad \forall t \in [a, b).$$

Then one has the estimate

$$u(t) \leq u_0 e^{\int_a^t \varphi(s) ds}, \quad \forall t \in [a, b).$$

Lemma 4.1.3 (*Gronwall lemma, classical version*)

Let $\varphi, \psi : [a, b) \rightarrow \mathbb{R}$ be two continuous functions on $[a, b) \subset \mathbb{R}$ and $u \in C^1([a, b))$. Let u satisfy moreover the following inequality

$$u'(t) \leq \psi(t) + \varphi(t) u(t), \quad \forall t \in [a, b).$$

Then one has the estimate

$$u(t) \leq u(0) e^{\int_a^t \varphi(s) ds} + \int_a^t \psi(s) e^{\int_s^t \varphi(\tau) d\tau} ds.$$

4.2 Poincaré inequality

Lemma 4.2.1 (Generalized Poincaré inequality) [24]

Let $\Omega \subset \mathbb{R}^d$ be an open, bounded domain with Lipschitz boundary. Furthermore, let us consider a continuous semi-norm

$$\mathcal{N} : W^{1,p}(\Omega) \rightarrow \mathbb{R}, \quad p \in [1, \infty).$$

Then, there exists a constant $C > 0$, depending only on Ω, n, p such that

$$\|u\|_{W^{1,p}(\Omega)} \leq C \left[\|\nabla u\|_{L^p(\Omega)} + \mathcal{N}(u) \right].$$

Remark 4.2.2 Some examples of continuous semi-norms are:

- $\mathcal{N}(u) := \int_{\Gamma} |u(x)| d\sigma$ with Ω of classe C^1 and $\Gamma \subset \partial\Omega$ with $|\Gamma| > 0$;
- $\mathcal{N}(u) := \langle u \rangle$ with $\langle u \rangle := \frac{1}{|\Omega|} \int_{\Omega} u dx$.

Lemma 4.2.3 (Poincaré-Wirtinger inequality) [10, 29]

Let $\Omega \subset \mathbb{R}^d$ be a connected open and bounded set of Lipschitz regularity and let $p \in [1, \infty]$. Then there exists a constant $C > 0$ depending only on Ω, n, p such that

$$\|u - \langle u \rangle\|_{L^p(\Omega)} \leq C \|\nabla u\|_{L^p(\Omega)}, \quad \forall u \in W^{1,p}(\Omega).$$

Lemma 4.2.4 (Inflow-Poincaré inequality) [10, 29]

Let $\Omega \subset \mathbb{R}^d$ be an open bounded set and let $p \in [1, \infty]$. Then there exists a constant $C > 0$ depending only on Ω, n, p such that

$$\|u\|_{L^p(\Omega)} \leq C \|\nabla u\|_{L^p(\Omega)}, \quad \forall u \in W_0^{1,p}(\Omega).$$

Remark 4.2.5 This last Poincaré inequality remains valid for domains which are bounded only in one direction (strip-like domains) or for functions which vanish only on part of the boundary $\Gamma \subset \partial\Omega$ with non-zero measure.

Lemma 4.2.6 (Weighted Poincaré inequality) [3]

Let us fix a sufficiently regular potential V satisfying

$$V \in L_{loc}^{\infty}(\mathbb{R}^d) \cap W_{loc}^{2,1}(\mathbb{R}^d), \quad \liminf_{|x| \rightarrow \infty} V(x) = \infty.$$

Then there exists some constant $C > 0$ such that

$$\int_{\mathbb{R}^d} |u|^2 e^{-V} dx \leq C \int_{\mathbb{R}^d} |\nabla u|^2 e^{-V} dx, \quad \forall u \in H^1(\mathbb{R}^d) \text{ such that } \int_{\mathbb{R}^d} u e^{-V} dx = 0.$$

Lemma 4.2.7 (Inhomogeneous Poincaré inequality) [28]

Let $\Omega := \mathbb{T} \times \mathbb{R}$ with \mathbb{T} the periodic torus in x , and let us consider the weighted measure $d\mu_{\infty} := \mathcal{M} dx dv$ where $\mathcal{M} := \frac{1}{\sqrt{2\pi}} e^{-v^2/2}$. Then, there exists some constant $C > 0$ depending only on Ω , such that for each $u \in H^1(d\mu_{\infty})$ satisfying $\int_{\Omega} u d\mu_{\infty} = 0$ one has

$$\int_{\Omega} |u|^2 d\mu_{\infty} \leq C \int_{\Omega} |\nabla u|^2 d\mu_{\infty}. \quad (4.1)$$

4.3 Logarithmic Sobolev inequalities

Lemma 4.3.1 (*Gaussian and Euclidean logarithmic Sobolev inequalities*)

Let $d\mu := \mathcal{M} dx$ be the normalized Gaussian measure on \mathbb{R}^d with $d \geq 1$ and $\mathcal{M}(x) := (2\pi)^{-d/2} e^{-|x|^2/2}$. The Gaussian logarithmic inequality reads then

$$\int_{\mathbb{R}^d} |\nabla u|^2 d\mu \geq \frac{1}{2} \int_{\mathbb{R}^d} |u|^2 \log(|u|^2) d\mu,$$

for all $u \in H^1(\mathbb{R}^d, d\mu)$ satisfying $\int_{\mathbb{R}^d} |u|^2 d\mu = 1$.

For $w := u \mathcal{M}^{1/2}$ we get $\int_{\mathbb{R}^d} |w|^2 dx = 1$, $\int_{\mathbb{R}^d} |x|^2 |w|^2 dx = d$ and via an integration by part we obtain the equivalent Euclidean logarithmic Sobolev inequality

$$\int_{\mathbb{R}^d} |\nabla w|^2 dx \geq \frac{1}{2} \int_{\mathbb{R}^d} |w|^2 \log(|w|^2) dx + \frac{d}{4} \log(2\pi e^2), \quad \forall w \in H^1(\mathbb{R}^d), w \geq 0, \|w\|_{L^2} = 1.$$

Lemma 4.3.2 [32] (*Convex Sobolev inequalities*)

Let $\phi : (0, \infty) \rightarrow [0, \infty)$ be a smooth function, such that

$$\phi(1) = 0, \quad \phi''(1) = 1, \quad \phi'' > 0, \quad (1/\phi'')'' \leq 0 \text{ on } (0, \infty).$$

The convex Sobolev inequality relates a non-negative convex entropy function

$$\mathcal{E}_\phi(u|u_\infty) := \int_{\mathbb{R}^d} \phi\left(\frac{u}{u_\infty}\right) u_\infty dx,$$

to an entropy-production function

$$\mathcal{I}_\phi(u|u_\infty) := - \int_{\mathbb{R}^d} \phi''\left(\frac{u}{u_\infty}\right) \left| \nabla \left(\frac{u}{u_\infty}\right) \right|^2 u_\infty dx,$$

in particular one has

$$\mathcal{E}_\phi(u|u_\infty) \leq \frac{1}{2} |\mathcal{I}_\phi(u|u_\infty)|,$$

for all $u : \mathbb{R}^d \rightarrow \mathbb{R}^+$ such that $u \in H^1(\mathbb{R}^d, d\mu)$ satisfying $\int_{\mathbb{R}^d} |u|^2 d\mu = 1$ with $d\mu := u_\infty dx$ and $u_\infty := (2\pi)^{-d/2} e^{-|x|^2/2}$, as well as $\int_{\mathbb{R}^d} u dx = 1$.

By choosing ϕ in a suitable way, we can obtain specific inequalities. For example, choosing the typical generating function $\phi(s) := s \log(s) - s + 1$ one gets

$$\int_{\mathbb{R}^d} u \log\left(\frac{u}{u_\infty}\right) dx \leq 2 \int_{\mathbb{R}^d} \left| \nabla \sqrt{\frac{u}{u_\infty}} \right|^2 u_\infty dx = \frac{1}{2} \int_{\mathbb{R}^d} u \left| \nabla \log\left(\frac{u}{u_\infty}\right) \right|^2 dx. \quad (4.2)$$

As one has $u_\infty := (2\pi)^{-d/2} e^{-|x|^2/2}$, the convex Sobolev inequality can be rewritten in the different form

$$\int_{\mathbb{R}^d} u \log(u) dx + \frac{d}{2} \log(2\pi) + d \leq 2 \int_{\mathbb{R}^d} |\nabla \sqrt{u}|^2 dx,$$

which is nothing else than the Euclidean logarithmic Sobolev inequality.

Remark 4.3.3 In bounded domains $\Omega \subset \mathbb{R}^d$ one has for some $C > 0$ (depending only on Ω and d) the following estimate, obtained from Sobolev injection and Poincaré-Wirtinger theorems

$$\int_{\Omega} u^2 \log\left(\frac{u^2}{\|u\|_{L^2(\Omega)}^2}\right) dx \leq C \|\nabla u\|_{L^2(\Omega)}^2 \quad \forall u \in H^1(\Omega).$$

4.4 Csiszár-Kullback inequality

The following inequality shows that the L^1 -distance of two functions f and g is controlled by the relative entropy

$$\mathcal{E}_\phi(f|g) := \int_{\Omega} \phi(f/g) g \, dx.$$

Lemma 4.4.1 [32] (*Classical Csiszár-Kullback inequality*)

Let $\Omega \subset \mathbb{R}^d$ be a domain and let $f, g \in L^1(\Omega)$ satisfy $f \geq 0$, $g > 0$ and $\int_{\Omega} f \, dx = \int_{\Omega} g \, dx = 1$. Let furthermore $\phi(s) := s \log(s) - s + 1$ for $s > 0$. Then, one has with optimal constant

$$\|f - g\|_{L^1}^2 \leq 2 \mathcal{E}_\phi(f|g).$$

Lemma 4.4.2 (*General Csiszár-Kullback inequality*)

Let $\Omega \subset \mathbb{R}^d$ be a domain and let $f, g \in L^1(\Omega)$ satisfy $f \geq 0$, $g > 0$ and $\int_{\Omega} f \, dx = \int_{\Omega} g \, dx = 1$. Let furthermore $\phi \in C^0([0, \infty)) \cap C^4(0, \infty)$ be such that $\phi(1) = 0$, $\phi''(1) > 0$, $\phi'''(1) > 0$, ϕ is convex and $1/\phi''$ is concave in $(0, \infty)$. Then, one has

$$\|f - g\|_{L^1}^2 \leq \frac{2}{\phi''(1)} \mathcal{E}_\phi(f|g).$$

Summary

The mathematical modelling and analysis of the collective behaviour of a cloud of N interacting particles or agents has attracted a lot of interest in the last years in several communities, such as biologists, physicists, mathematicians, computer scientists *etc.* This is motivated not only by fundamental reasons, such as the understanding of the natural phenomena occurring around us, but also by the wide applications of this field in several domains, such as collective robotics, unmanned areal vehicles, ...

Several mathematical models appeared in literature in the last years, such as for ex. the Viscek model, the Kuramoto model, the Cucker-Smale model *etc.*, each one being specifically adapted for a particular situation, and several mathematical and numerical studies have been performed, the literature being constantly growing. The basic models have been fully understood today, what is still open in our opinion is the design of more realistic models, permitting to get closer to reality, and the corresponding mathematical and numerical analysis. In fact, a truly good model must on one hand recreate the real-life behaviour one is investigating, and on the other hand it must be simple enough to enable a detailed mathematical and numerical study. So in our particular case of a drone swarm, all the specificities mentionned in Section 3.2 shall be step by step included in a realistic drone model and efficient, multi-scale numerical schemes designed to be proposed to the industrials.

Bibliography

- [1] Pedro Aceves-Sánchez, Mihai Bostan, Jose-Antonio Carrillo, Pierre Degond. *Hydrodynamic limits for kinetic flocking models of Cucker-Smale type* J. Mathematical Biosciences and Engineering, 2019, **16** (6): 7883-7910.
- [2] Achleitner, F., Arnold, A., & Carlen, E.A. (2017). On multi-dimensional hypocoercive BGK models. arXiv: Analysis of PDEs.
- [3] L. Addala, J. Dolbeault, X. Li, L.M. Tayeb *L2-Hypocoercivity and large time asymptotics of the linearized Vlasov-Poisson-Fokker-Planck system*, preprint.
- [4] S.M. Ahn, H. Choi, S.-Y. Ha, H. Lee *On collision-avoiding initial configurations to Cucker-Smale type flocking models*, CMS (Comm. in Math. Sci.) **10** (2012), no. 2, 625–643.
- [5] Albritton, D., Armstrong, S., Mourrat, J., & Novack, M. (2019). *Variational methods for the kinetic Fokker-Planck equation*. arXiv: Analysis of PDEs.
- [6] Arnold, Anton & Markowich, Peter & Toscani, Giuseppe & Unterreiter, Andreas. *On convex Sobolev inequalities and the rate of convergence to equilibrium for Fokker-Planck type equations*. 1999 Communications in Partial Differential Equations, 26:1-2, 43-100.
- [7] François Bolley, José A. Cañizo, José A. Carrillo, *Mean-field limit for the stochastic Vicsek model*, Applied Mathematics Letters, **25**, 3, 2012, 339-343.
- [8] Bostan, Mihai and José Antonio Carrillo. *Asymptotic Fixed-Speed Reduced Dynamics for Kinetic Equations in Swarming*. Mathematical Models and Methods in Applied Sciences **23** (2012), 2353-2393.
- [9] F. Bouchut, S. Jin, X. Li *Numerical approximations of pressureless and isothermal gas dynamics* SIAM Journal on Numerical Analysis, **41** (2003), 135–158.
- [10] H. Brezis, “Analyse Fonctionnelle”, Masson, Paris, 1983.
- [11] S. Camazine, J.-L. Deneubourg, N.R. Franks, J. Sneyd, G. Theraula, E. Bonabeau *Self-Organization in Biological Systems*, Princeton University Press, 2003.
- [12] F. Cao, S. Motsch, A. Reamy, R. Theisen *Asymptotic flocking for the three-zone model*, Mathematical Biosciences and Engineering **17** (2020), 7692–7707.

- [13] Carrapatoso, K., Dolbeault, J., Hérau, F., et al., *Special macroscopic modes and hypocoercivity*, 2021, arXiv:2105.04855. doi:10.48550/arXiv.2105.04855
- [14] J. A. Carrillo, M. Fornasier, G. Toscani, F. Vecil *Particle, kinetic, and hydrodynamic models of swarming*, Mathematical Modeling of Collective Behavior in Socio-Economic and Life Sciences (2010), 297–336.
- [15] Carrillo, J.A., Choi, YP. Mean-Field Limits: From Particle Descriptions to Macroscopic Equations. Arch Rational Mech Anal 241, 1529–1573 (2021).
- [16] J. A. Carrillo, Y.-P. Choi, P.B. Mucha, J. Peszek *Sharp conditions to avoid collisions in singular Cucker–Smale interactions*, Nonlinear Analysis: Real World Applications **37** (2017), 317–328.
- [17] J. A. Carrillo, A. Colombi, M. Scianna *Adhesion and volume constraints via nonlocal interactions determine cell organisation and migration profiles*, J. of Theoretical Biology **445** (2018), 75–91.
- [18] F. Cucker, S. Smale *Emergent Behavior in Flocks*, IEEE Transactions on Automatic Control **52** (2007), no. 5, 852–862.
- [19] F. Cucker, S. Smale *On the mathematics of emergence*, Japanese Journal of Mathematics **2** (2007), 197–227.
- [20] Degond, P., Frouvelle, A. & Liu, JG. *Macroscopic Limits and Phase Transition in a System of Self-propelled Particles*. Journal of Nonlinear Science **23** (2013), 427–456.
- [21] P. Degond, S. Motsch *Large-scale dynamics of the persistent turning walker model of fish behavior*, J. of Stat. Phys. **131** (2008), 989–1021.
- [22] P. Degond, S. Motsch *Continuum limit of self-driven particles with orientation interaction*, Mathematical Models and Methods in Applied Sciences **18** (2008), 1193–1215.
- [23] P. Degond, S. Motsch *Macroscopic limit of self-driven particles with orientation interaction*, C. R. Acad. Sci. Paris, Ser I. **345** (2007), 555–560.
- [24] F. Demengel, G. Demengel, *Espaces fonctionnels*, EDP Sciences, (2007).
- [25] L. Desvillettes, C. Villani *On the trend to global equilibrium for spatially inhomogeneous kinetic systems: The Boltzmann equation*, Inventiones mathematicae **159** (2005), 245–316.
- [26] Dietert, H. & Fernandez, B., *The mathematics of asymptotic stability in the Kuramoto model* Proceedings of the Royal Society of London Series A, **474** (2018), 20180467.
- [27] Dolbeault, J., Mouhot, C., & Schmeiser, C. (2010). *Hypocoercivity for linear kinetic equations conserving mass*. Transactions of the American Mathematical Society, 367, 3807–3828.

- [28] G. Dujardin, F. Héreau, P. Lafitte *Coercivity, hypocoercivity, exponential time decay and simulations for discrete Fokker-Planck equations*, *Numerische Mathematik* **144** (2020), 615–697.
- [29] L.C. Evans, *Partial Differential equations*, American Mathematical Society, (2010).
- [30] S.-Y. Ha, J.-G. Liu *A simple proof of the Cucker-Smale flocking dynamics and mean-field limit*, *CMS (Comm. in Math. Sci.)* **7** (2009), no. 2, 297–325.
- [31] F. Héreau *Introduction to hypocoercive methods and applications for simple linear inhomogeneous kinetic models*, *Analysis of Nonlinear Partial Differential Equations* **5** (2017), 119–147.
- [32] A. Jüngel *Entropy dissipation methods for nonlinear PDEs*, Lecture Notes, Spring School, Bielefeld, 2012.
- [33] Kolokolnikov T., Carrillo J.A., Bertozzi A., Fetecau R., Lewis M., *Emergent behaviour in multi-particle systems with non-local interactions*, *Physica D: Nonlinear Phenomena*, **260**, 2013, Pages 1-4,
- [34] Kuramoto Y. (1984) *Chemical oscillations, waves and turbulence*. New York, NY: Springer.
- [35] Kuramoto Y. (1975) Self-entrainment of a population of coupled nonlinear oscillators. In *Int. Symp. on Mathematical Problems in Theoretical Physics: January 23–29, 1975, Kyoto University, Kyoto, Japan* (ed. H Araki). *Lecture Notes in Physics*, vol. 39, pp. 420–422. Berlin, Germany: Springer
- [36] J.K. Parrish, S.V. Viscido, D. Grunbaum, *Self-organized fish schools: an examination of emergent properties*, *Biol. Bull.* **202** (2002), no. 3, 296–305.
- [37] J. Peszek *Existence of piecewise weak solutions of a discrete Cucker–Smale’s flocking model with a singular communication weight*, *J. Differential Equations* **257** (2014), no. 8, 2900–2925.
- [38] J. Peszek *Discrete Cucker-Smale flocking model with a weakly singular weight*, *SIAM J. Math. Anal.* **47** (2015), no.5, 3671–3686.
- [39] T. Vicsek et al. *Novel Type of Phase Transition in a System of Self-Driven Particles*, *Phys. Rev. Letters* **75** (1995), 1226–1229.
- [40] Cédric Villani. *Hypocoercivity*. *Mem. Amer. Math. Soc.*, **202** (950), 2009.
- [41] <https://sciencenorway.no/animals-plants-forskningno-norway/how-did-birds-first-begin-to-fly/1460173>
- [42] <http://bionotes.ru/biologiya/makrel-i-skumbriya>
- [43] <https://www.britannica.com/place/Serengeti-National-Park>
- [44] <https://www.epfl.ch/labs/lis/research/aerial-robotics>

- [45] <https://www.geoado.com/actus/des-robots-volants-pour-remplacer-les-abeilles-94317>
- [46] <https://fr.wikipedia.org/wiki/Fichier:Patrouille-de-france-virage-tricolore-a-8.jpg>
- [47] <https://blogs.unimelb.edu.au/sciencecommunication/2014/09/06/birdphysics>